DOE Award: DE-SC0019357
Title: Gene regulatory networks controlling carbohydrate selective deconstruction pathways in fungi
Awardee: Trustees of Clark University, Worcester, MA
PI: David S. Hibbett

Summary of Findings:

The Hibbett laboratory participated in a collaborative research project led by Dr. Jonathan Schilling (University of Minnesota), which sought to understand the genetic basis of lignocellulose decomposition in wood-decaying Agaricomycetes (mushroom-forming fungi), specifically "brown rot" species. The Hibbett laboratory contributed to this work principally by advising the Schilling laboratory on selection of strains for experimental analysis, based on evolutionary relationships of the fungi.

The Hibbett laboratory also conducted complementary studies of gene expression in wood-decaying Agaricomycetes. Four articles describing this work were produced (listed below). Wu et al. (2018) and Wu et al. (2019) described the impact of different substrates and types of culture media (solid media vs. sawdust suspended in liquid media). Wu et al. (2018) studied the brown rot species *Fomitopsis pinicola*, finding that gene expression was altered by both host species and culture conditions. Wu et al. (2019) extended the analysis to six species of closely related brown rot fungi, which again showed substrate-specific effects on gene expression. These results are of significance to other mechanistic studies on wood decay, because they indicate results obtained under one set of conditions may not be generalized to all conditions. Sabat et al. (2022) demonstrated that the composition of the secreted proteome of *F. pinicola* is also sensitive to substrate species (aspen vs. pine, in liquid cultures). Specifically, 30 carbohydrate active enzymes (CAZys) were more abundant on aspen vs. pine substrates, which corroborated the RNAseq results reported by Wu et al. (2018).

Wu et al. (2018) and Wu et al. (2019) also suggested that substrate-specific RNA editing occurs. However, a reanalysis of their data indicated that inferences about RNA editing were erroneous, because of technical problems in the analysis (specifically, RNAseq data were mapped to the assembled genomes, rather than to raw genomic reads, which caused errors in the genome assembly to appear as RNA editing events). A technical comment on these results and other reports of RNA editing in fungi was presented in Min et al. (2021).

The Hibbett laboratory also studied genes encoding plant cell wall degrading enzymes in 24 genomes representing eight described species and several unnamed lineages of the shiitake genus *Lentinula*, which is a group of white rot Agaricomycetes. The numbers and composition of CAZy genes in species of *Lentinula* (477, average) were not significantly different (P value of rank-sum test: 0.52), reflecting their conserved ecological role as white rot saprotrophs on hardwood substrates. A publication is currently under review (Sierra-Patev et al., in review).

Works cited (chronological):

Wu, Baojun, Jill Gaskell, Benjamin Held, Cristina Toapanta, Thu Vuong, Steven Ahrendt, Anna Lipzen, Jiwei Zhang, Jonathan Schilling, Emma Master, Igor Grigoriev, Robert Blanchette, Daniel Cullen, and David Hibbett. 2018. Substrate-Specific Differential Gene Expression and RNA editing in the Brown Rot Fungus *Fomitopsis pinicola*. Applied and Environmental Microbiology 84(16): e00991-18.

Wu, Baojun, Jill Gaskell , Jiwei Zhang, Cristina Toapanta, Steven Ahrendt, Igor V. Grigoriev, Robert Blanchette, Jonathan Schilling, Emma Master, Daniel Cullen, and David Hibbett. 2019. Evolution of substrate-specific gene

expression and RNA editing in brown rot wood-decaying fungi. The ISME Journal. Vol. 13 https:// doi.org/10.1038/s 41396-019-0359-2.

Min, Byougnam, Baojun Wu, Jill Gaskell, Jiwei Zhang, Christina Toapanta, Steven Ahrendt, Robert A. Blanchette, Emma Master, Daniel Cullen, David S. Hibbett, and Igor V. Grigoriev. 2021. RNA editing in Basidiomycota revisited. ISME Communications 1, 70. https://doi.org/10.1038/s43705-021

Grzegorz Sabat, Steven Ahrendt, Baojun Wu, Jill Gaskell, Benjamin W. Held, Cristina Toapanta, Thu V. Vuong, Anna Lipzen, Jiwei Zhang, Jonathan S. Schilling, Emma Master, Igor V. Grigoriev, Robert A. Blanchett, David S. Hibbett, Jennifer Bhatnagar, Daniel Cullen. 2022. Proteome of the wood decay fungus *Fomitopsis pinicola* is altered by substrate. Microbiology Resource Announcements 11; DOI: https://doi.org/ 10.1128/mra.00586-22

Sean Sierra-Patev, Byoungnam Min, Miguel Naranjo-Ortiz, Brian Looney, Zachary Konkel, Jason C. Slot, Yuichi Sakamoto,Jacob L. Steenwyk, Antonis Rokas, Juan Carro, Susana Camarero, Patricia Ferreira, Gonzalo Molpeceres, Francisco J. Ruiz-Dueñas, Ana Serrano, Bernard Henrissat, Elodie Drula, Karen W. Hughes, Juan L. Mata, Noemia Kazue Ishikawa, Ruby Vargas-Isla, Shuji Ushijima, Chris A. Smith, Steven Ahrendt, Willian Andreopoulos, Guifen He, Kurt LaButti, Anna Lipzen, Vivian Ng, Robert Riley, Laura Sandor, Kerrie Barry, Angel T. Martínez, Yang Xiao, John G. Gibbons, Kazuhisa Terashima, Igor V. Grigoriev, and David Hibbett. A Global Phylogenomic Analysis of the Shiitake Genus *Lentinula* (PNAS, in review).

Acknowledgement of Government Support and Government License

This work was generated with financial support from the U.S. Government through Contract/Award No. DE-SC0019357, and as such the U.S. Government retains a paid-up, nonexclusive, irrevocable, world-wide license to reproduce, prepare derivative works, distribute copies to the public, and display publicly, by or on behalf of the Government, this work in whole or in part, or otherwise use the work for Federal purposes.

AMERICAN SOCIETY FOR MICROBIOLOGY | Applied and Environmental Microbiology®

ENVIRONMENTAL MICROBIOLOGY

Retracted and Republished from: "Substrate-Specific Differential Gene Expression and RNA Editing in the Brown Rot Fungus *Fomitopsis pinicola*"

Baojun Wu,[a] Jill Gaskell,[b] Benjamin W. Held,[c] Cristina Toapanta,[c] Thu V. Vuong,[d] Steven Ahrendt,[e,f] Anna Lipzen,[e] Jiwei Zhang,[g] Jonathan S. Schilling,[g] Emma Master,[d] Igor V. Grigoriev,[e,f] Robert A. Blanchette,[c] Dan Cullen,[b] David S. Hibbett[a]

[a]Biology Department, Clark University, Worcester, Massachusetts, USA
[b]USDA Forest Products Laboratory, Madison, Wisconsin, USA
[c]Department of Plant Pathology, University of Minnesota, St. Paul, Minnesota, USA
[d]Department of Chemical Engineering and Applied Chemistry, University of Toronto, Toronto, Ontario, Canada
[e]Department of Energy, Joint Genome Institute, Walnut Creek, California, USA
[f]Department of Plant and Microbial Biology, University of California, Berkeley, California, USA
[g]Department of Plant and Microbial Biology, University of Minnesota, St. Paul, Minnesota, USA

PUBLISHER'S NOTE The American Society for Microbiology and *Applied and Environmental Microbiology* would like to inform the readers that this article is a corrected and republished version of https://doi.org/10.1128/AEM.00991-18, which was retracted (https://doi.org/10.1128/AEM.00330-21). As stated in the retraction notice, after publication, the authors performed additional analyses and "discovered that the RNA editing results (but not the gene expression results) are artifactual." Thus, one of the main conclusions of the original paper can no longer be supported, but the conclusions around the "substrate-specific differential gene expression" continue to be validated and described in this paper. Therefore, the authors were allowed to submit an entire, corrected manuscript for consideration to the journal. The manuscript was peer reviewed and subsequently accepted.

ABSTRACT Wood-decaying fungi tend to have characteristic substrate ranges that partly define their ecological niche. *Fomitopsis pinicola* is a brown rot species of Polyporales that is reported on 82 species of softwoods and 42 species of hardwoods. We analyzed gene expression levels of *F. pinicola* from submerged cultures with ground wood powder (sampled at 5 days) or solid wood wafers (sampled at 10 and 30 days), using aspen, pine, and spruce substrates (aspen was used only in submerged cultures). *Fomitopsis pinicola* expressed similar sets of wood-degrading enzymes typical of brown rot fungi across all culture conditions and time points. Nevertheless, differential gene expression was observed across all pairwise comparisons of substrates and time points. Genes exhibiting differential expression encode diverse enzymes with known or potential function in brown rot decay, including laccase, benzoquinone reductase, aryl alcohol oxidase, cytochrome P450s, and various glycoside hydrolases. Comparing transcriptomes from submerged cultures and wood wafers, we found that culture conditions had a greater impact on global expression profiles than substrate wood species. These findings highlight the need for standardization of culture conditions in studies of gene expression in wood-decaying fungi.

IMPORTANCE All species of wood-decaying fungi occur on a characteristic range of substrates (host plants), which may be broad or narrow. Understanding the mechanisms that allow fungi to grow on particular substrates is important for both fungal ecology and applied uses of different feedstocks in industrial processes. We grew the wood-decaying polypore *Fomitopsis pinicola* on three different wood species—aspen, pine, and

Citation Wu B, Gaskell J, Held BW, Toapanta C, Vuong TV, Ahrendt S, Lipzen A, Zhang J, Schilling JS, Master E, Grigoriev IV, Blanchette RA, Cullen D, Hibbett DS. 2021. Substrate-specific differential gene expression in the brown rot fungus *Fomitopsis pinicola* (Retracted and republished from: "Substrate-specific differential gene expression and RNA editing in the brown rot fungus *Fomitopsis pinicola*"). Appl Environ Microbiol 87:e00329-21. https://doi.org/10.1128/AEM.00329-21.

Editor Maia Kivisaar, University of Tartu

Address correspondence to David S. Hibbett, dhibbett@clarku.edu.

Received 13 February 2021
Accepted 28 April 2021
Published 27 July 2021

spruce—under various culture conditions. We found that *F. pinicola* is able to modify gene expression (transcription levels) across different substrate species and culture conditions. Many of the genes involved encode enzymes with known or predicted functions in wood decay. This study provides clues to how wood-decaying fungi may adjust their arsenal of decay enzymes to accommodate different host substrates.

KEYWORDS basidiomycetes, decay, lignocellulose, transcriptome, Polyporales, brown rot

Wood (lignocellulose) is one of the most abundant carbon pools in terrestrial ecosystems. Decomposition of wood is a critical component of the carbon cycle and may be exploited in the production of biofuels and other technologies. The most abundant and best-studied wood-decaying organisms are Agaricomycetes (Basidiomycota) (1–5). Most wood-decaying Agaricomycetes can be placed into one of two major decay categories: (1) white rot, in which all components of plant cell walls are degraded, including the highly recalcitrant lignin fraction, and (2) brown rot, in which lignin is modified but not appreciably removed (6–8). Phylogenomic analyses have demonstrated that brown rot fungi have evolved repeatedly from white rot ancestors (9–11).

Evolution of brown rot is associated with extensive losses of genes encoding plant cell wall-degrading enzymes, including peroxidases, laccases, and other ligninolytic oxidases, as well as carbohydrate-active enzymes (CAZymes), such as glycoside hydrolases (GHs), carbohydrate esterases (CEs), and lytic polysaccharide monooxygenases (LPMOs), coupled with reductions in cellulose-binding modules (CBM1s) associated with diverse CAZymes. Nevertheless, brown rot fungi cause rapid loss of strength and mass in wood substrates (6, 7, 12–14). The model brown rot fungus *Rhodonia placenta* (here referred to as *Postia placenta*, to maintain continuity with prior literature) appears to attack wood cell walls in a two-step process, in which reactive oxygen species are first deployed to effect an oxidative pretreatment of lignocellulose, followed by action of GHs that break down cellulose and hemicellulose into assimilable sugars, leaving lignin as a modified polymeric residue (15–17).

Most species of wood-decaying Agaricomycetes have characteristic substrate ranges that define their ecological activity in forest ecosystems and which can be useful for identification purposes (18–20). Brown rot species have been suggested to preferentially decay softwoods (gymnosperms, particularly Pinaceae), although many also attack hardwoods (angiosperms) (21, 22). The hemicellulose and lignin composition of hardwoods and softwoods differ and may affect substrate preferences by fungi. The hemicellulose of hardwoods is enriched in glucuronoxylan, whereas the main hemicellulose of softwoods is galactoglucomannan, and the lignin fraction of softwood is mainly guaiacyl lignin, whereas hardwoods have a larger (but variable) fraction of syringyl lignin (23–25). Secondary metabolite profiles also differ, with softwoods containing large amounts of terpenes and other extractives and hardwoods being highly variable in extractive compounds (24).

The mechanism(s) of brown rot decay remain uncertain, but hydroxyl radicals have been implicated as the diffusible oxidants (26, 27). Fenton chemistry ($H_2O_2 + Fe^{2+} + H^+ \rightarrow H_2O + Fe^{3+} + \cdot OH$) has been proposed, and three models are often cited (4, 28). A central role for cellobiose dehydrogenase had been proposed, but it is now clear that some brown rot fungi that efficiently cause extensive decay, such as *P. placenta* and *Wolfiporia cocos*, lack the gene for this enzyme (29). Alternatively, certain low-molecular-weight glycopeptides (GLPs) are thought to reduce extracellular Fe^{3+} in white and brown rot fungi (30–33). Perhaps the most widely held model involves hydroquinone cycling (34–36), which generates both Fenton reactants through the activities of a quinone reductase and oxalate-Fe^{3+} chelates. Several studies have suggested that laccases may also be involved in hydroquinone oxidation (37–39). Regardless of the mechanism(s), brown rot is thought to involve sequential oxidation and hydrolysis of lignocellulose.

Numerous studies have demonstrated the impact of culture conditions on transcript and protein accumulation levels in wood decay fungi (29, 40–42), including comparisons of expression on defined media (e.g., glucose, maltose, or crystalline cellulose) versus wood as a carbon

source or under aerobic or anaerobic conditions (43–48). However, there have been relatively few side-by-side comparisons of gene expression on different wood species (43, 49–57).

Several prior transcriptomic analyses concluded that wood decay fungi express similar sets of plant cell wall-degrading enzymes on both hardwood and softwood, although there may be disparities in the expression of individual genes on different substrates (43, 50, 51, 53, 56). For example, Vanden Wymelenberg et al. (56) found that 47 genes in the model white rot fungus *Phanerochaete chrysosporium* were upregulated >2-fold on aspen versus pine, including 13 genes encoding GHs, while in *P. placenta* 164 genes showed differential expression on the two substrates (roughly equal numbers upregulated on each substrate). The *P. placenta* genes upregulated on pine included 15 genes encoding cytochrome P450s, which are thought to play a role in the degradation of complex wood extractives (29, 58, 59). Similarly, Gaskell et al. (50) detected three P450s upregulated on pine versus aspen in another brown rot species, *Wolfiporia cocos*. A comparison of the genome of *P. chrysosporium* with the closely related *Phanerochaete carnosa* demonstrated an expansion of P450s in the latter species, which is almost exclusively collected on conifer wood (54). Moreover, *P. carnosa* was shown to transform a higher fraction of phenolics from heartwood than *P. chrysosporium* (54), consistent with the view that P450s play a role in detoxifying wood extractives. Couturier et al. (43) also found that eight genes encoding P450s in another white rot fungus, *Pycnoporus coccineus*, were differentially expressed on pine versus aspen. Genes encoding other enzymes active in lignocellulose digestion that have been shown to be differentially expressed on hardwoods versus softwoods include those encoding LPMOs, manganese peroxidases (MnP), lignin peroxidases (LiP), GH10 xylanases, and GH78 α-L-rhamnosidase (43, 50, 52).

It is difficult to make generalizations from the results of previous studies comparing gene expression on different substrates because their experimental conditions and organisms are highly variable. Most studies have used submerged milled wood substrates (43, 50, 52, 53, 56, 60), but others have used solid wood wafers (49) or sawdust (54, 55). Sampling times in studies using submerged substrates range from 3 days (43) to 16 days (53), while studies using sawdust or wood wafers have sampled at 10 days (49) to 42 days (54). About a dozen different tree species have been used as experimental substrates. The most commonly used hardwood is aspen (*Populus tremuloides* and *P. grandidentata*), including transgenic and hybrid lines with various lignin contents (49, 50, 60), but sugar maple (*Acer saccharum*) and yellow birch (*Betula alleghaniensis*) have also been employed (51, 52, 54). Softwood substrates include fir (*Abies balsamea*), three species of spruce (*Picea abies*, *P. glauca*, and *P. rubens*), and five pines (*Pinus contorta*, *P. halepensis*, *P. resinosa*, *P. strobus*, and *P. sylvestris*) (43, 50–54, 56). Yakovlev et al. (55) compared results on heartwood, reaction wood, and sapwood of *P. abies* and *P. sylvestris*.

The most commonly studied fungal species in analyses of substrate-specific gene expression are white rot species of the Polyporales, particularly *P. chrysosporium* and *P. carnosa* (49, 51, 52, 54, 56, 60). Other white rot species that have been studied include *Pycnoporus cinnabarinus* and *Dichomitus squalens* (43, 53), which are both in the Polyporales, and *Heterobasidion annosum*, which is in the Russulales (55). Two brown rot species of Polyporales, *P. placenta* and *W. cocos*, have been used in studies comparing gene expression on different tree species, specifically aspen and pine (49, 50, 56).

Here, we present an analysis of substrate-specific responses in *Fomitopsis pinicola*, which is a brown rot wood-decaying species of Polyporales that is reported to occur on 82 species of gymnosperms (softwoods), most commonly on pines and spruces, as well as 42 species of angiosperms (hardwoods), including aspen, birch, and cherry (61). This diverse range of substrates suggests that *F. pinicola* may have the ability to adjust its arsenal of decay enzymes according to the chemistry and anatomy of different hosts. *F. pinicola*, *P. placenta*, and *W. cocos* are members of the informally named "*Antrodia* clade," which includes diverse brown rot species. The *Antrodia* clade is

strongly supported as a monophyletic group (10), suggesting that the brown rot decay mechanisms of *F. pinicola*, *P. placenta*, and *W. cocos* are homologous.

We obtained results at one time point on three substrates (pine, spruce, and aspen) in submerged cultures and at two time points on two substrates (pine and spruce) on wood wafers. Thus, our results allow us to assess the impact of substrate wood species versus culture conditions on transcription.

RESULTS

Expression profiling of *F. pinicola* grown in submerged culture. Cultures of *F. pinicola* were grown in submerged cultures supplemented with ground aspen, pine, or spruce as the sole carbon source for 5 days. Owing to the accessibility of the substrate, rapid growth of wood decay fungi is typically observed under these conditions (29, 47, 49, 60, 62–64). Transcript levels and patterns of expression observed here support the involvement of numerous genes in lignocellulose degradation.

The highest transcript levels corresponded to the same genes in all three substrates. Not surprisingly, putative "housekeeping" genes such as short-chain dehydrogenase/reductases (SDR), ADT/ATP carriers, and a FAD/NAD domain ranked among the 30 highest FPKM (fragments per kilobase per million) values (Table 1; see also Table S1). Genes encoding glycoside hydrolases and carbohydrate esterases (GH18, GH128, GH78, CE4, and CE6), broadly categorized as hemicellulases, were also highly expressed, especially those with predicted secretion signals. This sharply contrasts with white rot fungi that express high levels of cellulose-attacking hydrolases (GH6s and GH7s) and lytic polysaccharide monooxygenases (LPMOs). Oligopeptide transporter and extracellular protease may reflect the importance of nitrogen scavenging in wood, whereas extracellular lipases likely facilitate triglyceride utilization.

Hierarchical clustering analysis based on expression levels revealed three groups corresponding to the substrates (see Fig. S1). Transcriptome profiles of *F. pinicola* with pine are more similar to those with aspen than spruce, which is surprising, because spruce and pine are softwoods (Pinaceae), whereas aspen is a hardwood. To verify transcriptome results, we performed qRT-PCR analyses of two differentially regulated genes. Consistent with RNA-seq, the expression patterns of *F. pinicola* with pine are more similar to those with aspen, and the lowest transcript levels of thaumatin-like protein (Fompi_110401) and a peptidase (Fompi_1113467) were observed in colonized pine and spruce, respectively (see Fig. S2).

Of the 13,885 genes predicted in the *F. pinicola* genome, 91 genes were differentially expressed (4-fold change and $P < 0.05$) among the three pairwise comparisons of substrates (aspen versus pine, aspen versus spruce, and pine versus spruce) in submerged culture (Fig. 1; see also Table S1). Consistent with the global expression pattern, fewer genes showed differential expression in pairwise comparisons between aspen and pine than in the other two pairwise comparisons (Fig. 1). GO enrichment analysis of upregulated genes on each substrate reveal very different terms for cellular component (CP), biological process (BP), and molecular function (MF) (Fig. 2), with none shared by all three substrates.

Eleven DEGs among the three pairwise comparisons encode enzymes with predicted functions in wood decay (Fig. 1, names in red). The expression levels of these genes were roughly clustered based on their putative function. These include laccase, benzoquinone reductase and aryl-alcohol oxidase (Fig. 1) possibly involved in the generation of hydroxyl radical via Fenton reactions (34–36, 39). In particular, benzoquinone reductase has been implicated in the redox cycling of Fe and H_2O_2, key Fenton reactants (35), and the process of hydroquinone oxidation may be augmented by laccases (39). While generally considered an oxidative process in brown rot, hydrolytic enzymes may also participate in cellulose degradation (65). Supporting this, a predicted endo-1,4-glucanase (Fig. 1) was expressed. Typical of brown rot fungi, this GH5_5 family protein lacks a cellulose binding module, and no exo-cellobiohydrolases occur within the *F. pinicola* genome. Thus, the importance of cellulose hydrolysis by conventional enzymes remains unclear. Differential expression analyses also revealed four genes encoding P450s, which are distributed among all three pairwise-substrate

TABLE 1 Thirty most abundant transcripts in submerged culture containing ground pine as the sole carbon source[a]

		Conditions						Protein	
Pro ID	Putative function[b]	Pine FPKM	Pine order	Spruce FPKM	Spruce order	Aspen FPKM	Aspen order	No. of TMHs	SP
Fompi_1030775	AA3_3, alcohol oxidase	12,993	1	10,068	1	11,821	1		
Fompi_1152048	Aquaporin-like	8,946	2	4,319	4	7,387	2	6	
Fompi_1039841	NAD-dependent formate dehydrogenase	6,013	3	7,407	2	5,516	3		
Fompi_49484	CipC protein	3,552	4	4,951	3	3,315	4		
Fompi_160683	GH18 protein	2,936	5	2,705	6	3,003	5		+
Fompi_1084629	Mannoprotein	2,811	6	2,639	7	2,870	6		+
Fompi_1022702	Glutamine-dependent formaldehyde dehydrogenase	2,588	7	2,896	5	2,452	8		
Fompi_1023896	ABC transporter	2,554	8	1,967	14	2,591	7		
Fompi_49935	NAD(P) binding SDR	2,236	9	2,257	9	1,912	11		
Fompi_1090124	Endosulfine-domain protein	2,105	10	1,338	20	2,167	9		
Fompi_1023614	Acid protease	1,816	11	2,240	10	2,129	10	1	+
Fompi_126349	MFS general substrate transporter	1,633	12	1,250	23	1,758	12	12	
Fompi_1021547	Lipase*	1,631	13	848	36	941	30		+
Fompi_1168917	NAD-dependent formate dehydrogenase	1,564	14	1,905	15	1,445	15		
Fompi_1022193	GH128 protein	1,529	15	1,514	17	1,527	13		+
Fompi_1147363	Catalase	1,484	16	1,336	21	1,172	22		
Fompi_1039147	General substrate transporter	1,417	17	2,204	11	1,253	19	12	
Fompi_159299	CE4-CBM50	1,367	18	1,449	18	1,419	17		+
Fompi_1023676	Peptidoglycan binding	1,357	19	1,448	19	1,489	14		+
Fompi_1022010	OPT oligopeptide transporter	1,313	20	869	33	968	27	16	
Fompi_129535	FAD/NAD(P)-binding domain	1,292	21	1,742	16	1,207	20		
Fompi_1131909	Aldehyde dehydrogenase	1,190	22	1,251	22	1,089	26		
Fompi_1021548	Lipase*	1,171	23	1,055	28	780	34	1	+
Fompi_145400	GH78	1,150	24	773	43	1,320	18		+
Fompi_1119394	CE6	1,070	25	1,053	29	1,180	21	1	+
Fompi_98853	GH16	1,064	26	916	31	1,140	24	1	
Fompi_1022048	Eukaryotic ADP/ATP carrier	1,029	27	1,145	26	1,122	25	3	
Fompi_1025554	SDR	1,012	28	890	32	950	29	2	
Fompi_59695	Hexose transporter	1,012	29	2,592	8	1,429	16	11	
Fompi_161955	SDR	962	30	1,187	25	880	31		

[a]Excludes genes designated "hypothetical" and those with no significant similarity to NCBI NR accession numbers. GH, glycoside hydrolase; CE, carbohydrate esterase; TMHs, predicted transmembrane helices; SP, predicted secretion signal; AA, auxiliary activities as described in the Carbohydrate Active Enzymes database (http://www.cazy.org/) (88, 89); SDR, short-chain dehydrogenase/reductase.

[b]*, Lipase genes tandemly linked ~2 kb apart.

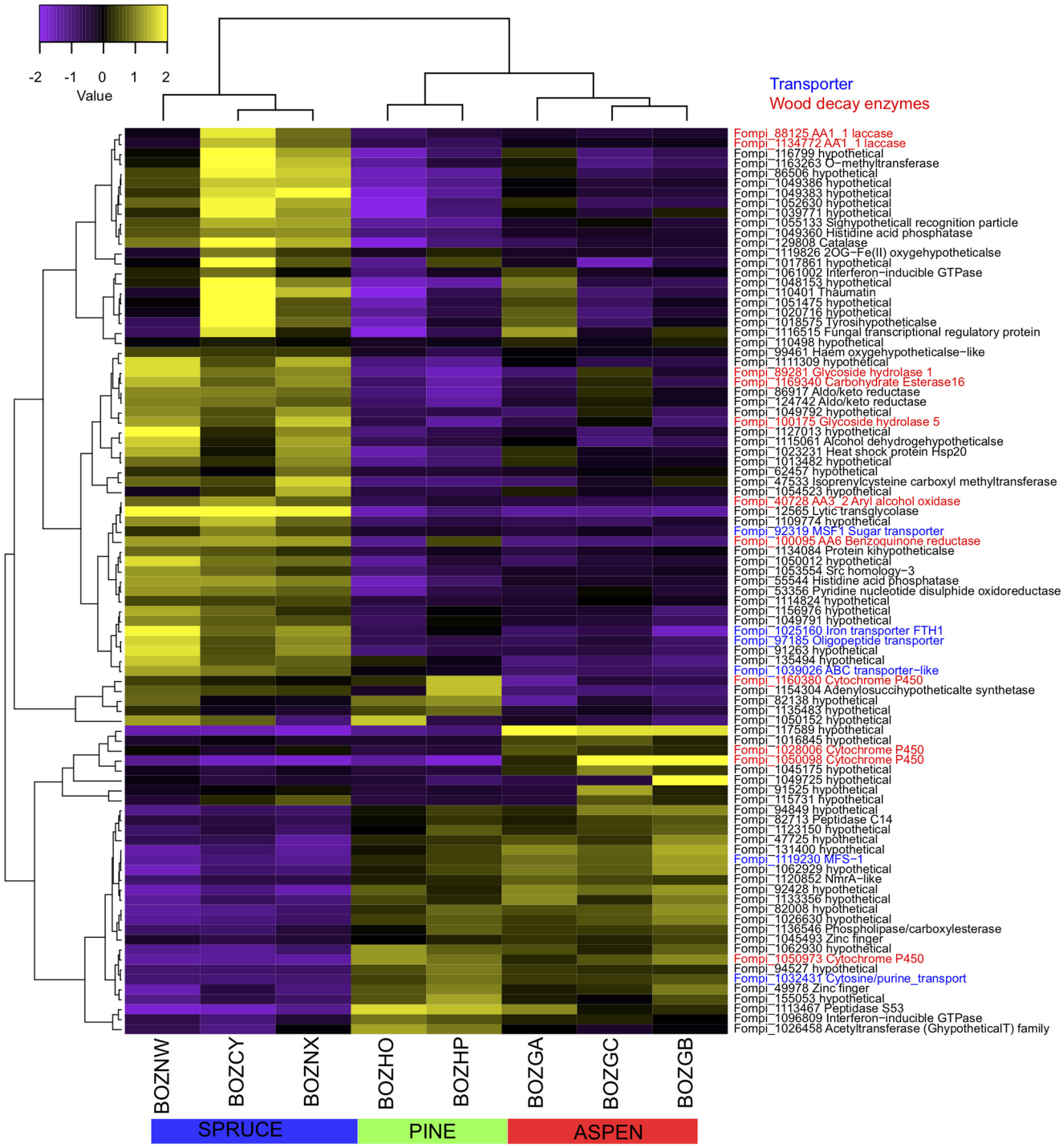

FIG 1 Heatmap showing hierarchical clustering of 11 genes with predicted functions in wood decay with a 4-fold change (FDR $<$ 0.05) in pairwise-substrate comparisons at day 5. The scale above the map shows $\log_2$-based signals under central row. Protein IDs and their enzyme names are indicated on the right side of the heatmap. Transporters are labeled in blue, and wood-decay enzymes are labeled in red. The bottom column designations refer to replicate libraries.

comparisons (Fig. 1). These may be involved in intracellular metabolism of low-molecular-weight breakdown products of lignin and resins (66, 67).

A previous study of *W. cocos* (50) indicated that membrane-bound proteins are potentially important for carbohydrate metabolism during wood decay. We found that 8% to 22% of DEGs from each pairwise comparison have transmembrane (TM) domains, including six transporters (Fig. 1), which may facilitate movement of small solutes across cell membranes.

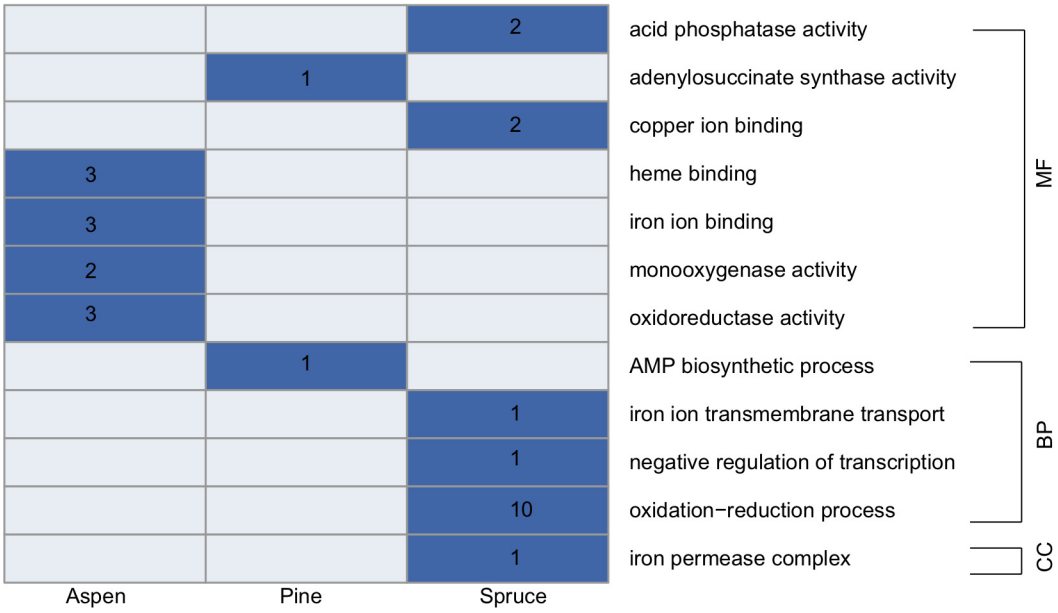

FIG 2 GO enrichment of upregulated genes from each substrate after 5-day-old submerged incubation. Categories of GO terms are labeled on the right side of the heatmap. Substrates are labeled at bottom of heatmap. Dark blue shading indicates presence, and light blue indicates absence. The genes number in each GO term was labeled in dark blue.

In addition, two proteins have functions related with methylation (Fompi_47533) and phosphorylation (Fompi_55544) (see Table S1), suggesting that modification of proteins might be involved during the decay process in submerged culture.

Expression profiling of *F. pinicola* grown on wood wafers. Submerged cultures and colonized wafers share many of the more highly expressed genes (Tables 1 and 2), including some that are likely involved in lignocellulose degradation. Among these are several glycosidases, a lipase (Fompi_1021547) potentially involved in fatty acid catabolism, and an alcohol oxidase (Fompi_1030775) similar to the methanol oxidase of *Gloeophyllum trabeum* (68). The latter enzyme has been implicated in the generation of peroxide from methanol during brown rot demethylation of lignin. The presence of proteins, as well as modifications of lignin and wood extractives, after 10 and 30 days of postinoculation was confirmed by time-of-flight secondary ion mass spectrometry (ToF-SIMS; for ToF-SIMS methods and results, see the supplemental material). The fungal treated wood samples, on both day 10 and day 30, were distinguished from the corresponding untreated samples by the abundance of protein-specific peaks, as well as the depletion of many extractive peaks, including 43, 55, and 67 Da (see Fig. S3). A closer look at the loadings of principal-component analysis also indicated the removal of generic aromatic peaks (see Fig. S3).

Time-dependent gene expression. Differentially expressed transcripts corresponding to 320 and 776 genes were identified by pairwise comparisons on pine and spruce, respectively (Fig. 3A; see also Table S2). DEGs showed different trajectories on different substrates. On pine, there were far fewer upregulated genes than downregulated genes at day 30 compared to day 10, whereas on spruce there were slightly more upregulated genes than downregulated genes on day 30 versus day 10 (Fig. 3A).

We performed enrichment analyses of upregulated DEGs from different time points on each substrate and found the enriched GO terms to be highly variable along the time course (Fig. 3B). The influence of incubation time is also pronounced among relative proportion of TM proteins (Fig. 4). MFS-1, cytochrome P450, and oligopeptide transporter are enriched after a 10-day incubation on pine but disappear after a 30-day incubation (Fig. 4B). Conversely, on spruce MFS-1 and cytochrome P450 are enriched at the later stage (Fig. 4C).

To evaluate the roles of carbohydrate-active enzymes and nonenzymatic oxidation reactions during the time course, we counted the number of CAZymes (GH, CE,

TABLE 2 Thirty most abundant transcripts in colonized spruce and pine wafers after 30 days[a]

		Conditions				Protein	
Pro ID	Putative function	Spruce-30D FPKM	Spruce order	Pine30 FPKM	Pine30 order	No. of TMHs	SP
Fompi_1152048	Aquaporin-like	5,523	1	6,517	1	6	
Fompi_1030775	AA3_3, alcohol oxidase	4,056	2	5,301	2		
Fompi_128521	L-Fuculose-phosphate aldolase	3,490	3	1,397	15		
Fompi_1021547	Lipase[b]	3,192	4	3,496	3		+
Fompi_1131909	Aldehyde dehydrogenase	1,808	5	1,586	8		
Fompi_1090124	Endosulfine-domain-containing protein	1,537	6	1,561	9		
Fompi_160683	GH18	1,493	7	1,451	13		+
Fompi_1025554	SDR	1,487	8	1,555	11	2	
Fompi_1022048	Mitochondrial carrier	1,454	9	1,503	12	3	
Fompi_1147363	Catalase	1,423	10	1,478	13		
Fompi_148786	CE4	1,383	11	751	50		+
Fompi_86900	MFS general substrate transporter	1,367	12	961	34	12	
Fompi_1044587	Plasma membrane proteolipid 3	1,365	13	989	30	2	
Fompi_1022193	Glycoside hydrolase family 128 protein	1,361	14	1,637	5		+
Fompi_1022498	Ribosomal protein S25	1,341	15	1,560	10		
Fompi_126349	MFS general substrate transporter	1,263	16	1,055	24	12	
Fompi_1025379	Peptidyl-prolyl *cis-trans* isomerase	1,245	17	1,003	28		
Fompi_113951	Ribosomal protein 60S	1,234	18	1,183	19		
Fompi_1021745	Polyubiquitin	1,232	19	1,354	16		
Fompi_1039841	NAD formate dehydrogenase	1,208	20	1,632	6		
Fompi_1022753	RNA-binding domain	1,161	21	969	33		
Fompi_127599	Actin 1	1,153	22	1,223	17		
Fompi_1112040	Histone H3	1,146	23	1,184	18		
Fompi_1023676	CBM50	1,088	24	995	29		+
Fompi_1025222	Manganese superoxide dismutase	1,078	25	627	63		
Fompi_56132	Acid protease	1,023	26	1,138	21		
Fompi_1028183	Acetohydroxy acid isomeroreductase	992	27	692	58		
Fompi_1142989	Ubiquitin/40S ribosomal protein fusion	983	28	1,024	27		
Fompi_84886	Thaumatin-like protein	957	29	572	74		+
Fompi_56163	GH5_9	955	30	822	42		+

[a]Excludes genes designated "hypothetical" and those with no significant similarity to NCBI NR accession numbers. GH, glycoside hydrolase; CE, carbohydrate esterase; TMH, predicted transmembrane helices; SP, predicted secretion signal; AA, auxiliary activities as described in the Carbohydrate Active Enzymes database (http://www.cazy.org/) (88, 89); SDR, short-chain dehydrogenase/reductase.

[b]Lipase genes tandemly linked ~2 kb apart.

and PL), various redox enzymes potentially involved in Fenton systems (AA family members, HTPs, oxalate metabolism, and iron homeostasis), and cytochrome P450s among the DEGs. For each category, only the upregulated gene at one time point relative to the other one was considered. On each substrate, the number of CAZymes decreased with increased incubation time, while the number of lignin-degrading enzymes increased (Fig. 3C; see also Table S3). In contrast, the cytochrome P450 transcript accumulation patterns are not consistent between substrates (Fig. 3C; see also Table S3). On pine, the trend of cytochrome P450 is consistent with the CAZymes, whereas the cytochrome P450 on spruce is consistent with that of lignin enzymes.

Based on comparisons to *P. chrysosporium* iron reducing glycopeptides (31, 33), 10 *F. pinicola* homologs were identified. Transcripts corresponding to Fompi_1027255 decreased over time in both pine and spruce. This expression pattern would be expected where initial stages of decay relied heavily on oxidative depolymerization of cellulose whereas later stages might shift toward hydrolytic mechanisms.

Substrate-dependent gene expression. We compared expression patterns on pine and spruce substrates at the same time points. A total of 294 DEGs were identified by substrate comparisons after a 10-day incubation, of which 199 were upregulated on pine, and 95 were upregulated on spruce (Fig. 3A; see also Table S2). After a 30-day incubation, 135 DEGs were identified on pine versus spruce, of which only 18 were substantially upregulated on pine (Fig. 3A; see also Table S2).

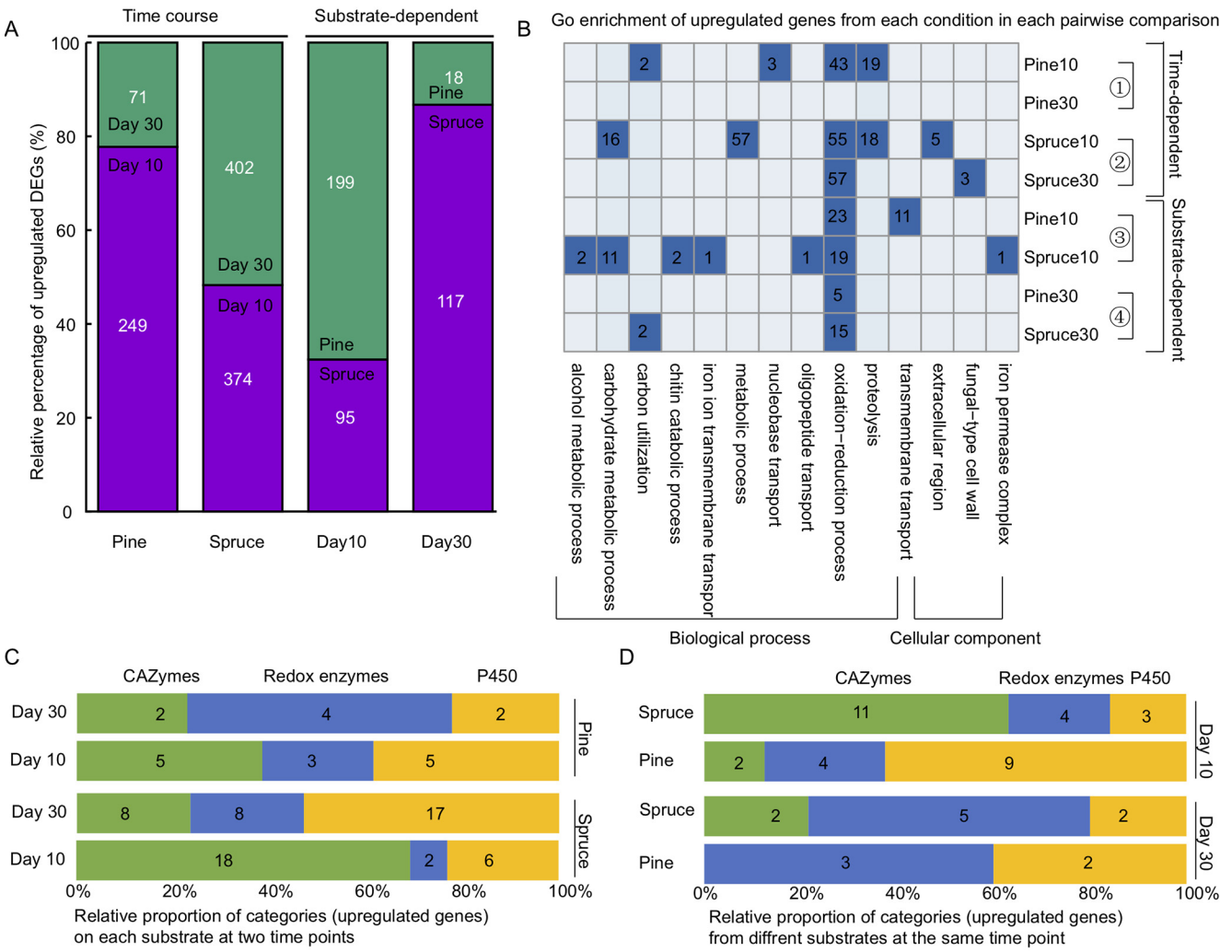

FIG 3 Differential expression of *F. pinicola* on different wood wafers (pine and spruce) after 10-day and 30-day incubations. (A) Relative percentage of upregulated DEGs on different substrates and at different time points. (B) GO enrichment of upregulated genes from each condition in each pairwise comparison. Four pairwise comparisons are labeled on the right side of the heatmap. Dark blue shading indicates presence, and light blue indicates absence. The number of genes in each GO term was labeled in dark blue. (C) Distribution in relative proportion of wood decay CAZymes (GH, CE, and PL), redox enzymes potentially involved in Fenton chemistry (AA families, HTP, POD, CRO, OXO, GLP, and QRD), and cytochrome P450s at different time points (C) and on different substrates (D). For each category, only the upregulated genes at one time point/substrate relative to the other time point/substrate was considered.

GO enrichment analysis of substrate-dependent upregulated genes after a 10-day incubation revealed six different biological processes and one different cellular component between pine and spruce. Most biological processes are enriched on spruce (Fig. 3B). The difference in enriched GO terms is diminished in the 30-day comparisons. After 10-day incubations, TM proteins, cytochrome P450, sugar transporter, and oligopeptide transporter are enriched on pine relative to spruce, while MFS-1 is enriched on spruce relative to pine after 30-day incubation (Fig. 4). CAZymes, AA enzymes, and cytochrome P450s were also explored between substrates. After a 10-day incubation, spruce-dependent upregulated genes include 5-fold more genes encoding CAZymes and one-third as many genes encoding cytochrome P450s relative to pine. However, there was no change in AA enzymes (Fig. 3D; see also Table S3). After a 30-day incubation, spruce-dependent upregulated genes included slightly more genes encoding AA and other CAZyme family members, compared to pine (Fig. 3D; see also Table S3).

Cross-culture method comparisons. We performed hierarchical clustering of gene expression patterns using samples from different substrates (pine versus spruce), time points (day 5, day 10, and day 30) and culture methods (submerged versus wood wafers). Samples from the same time points and culture methods clustered with each other, regardless

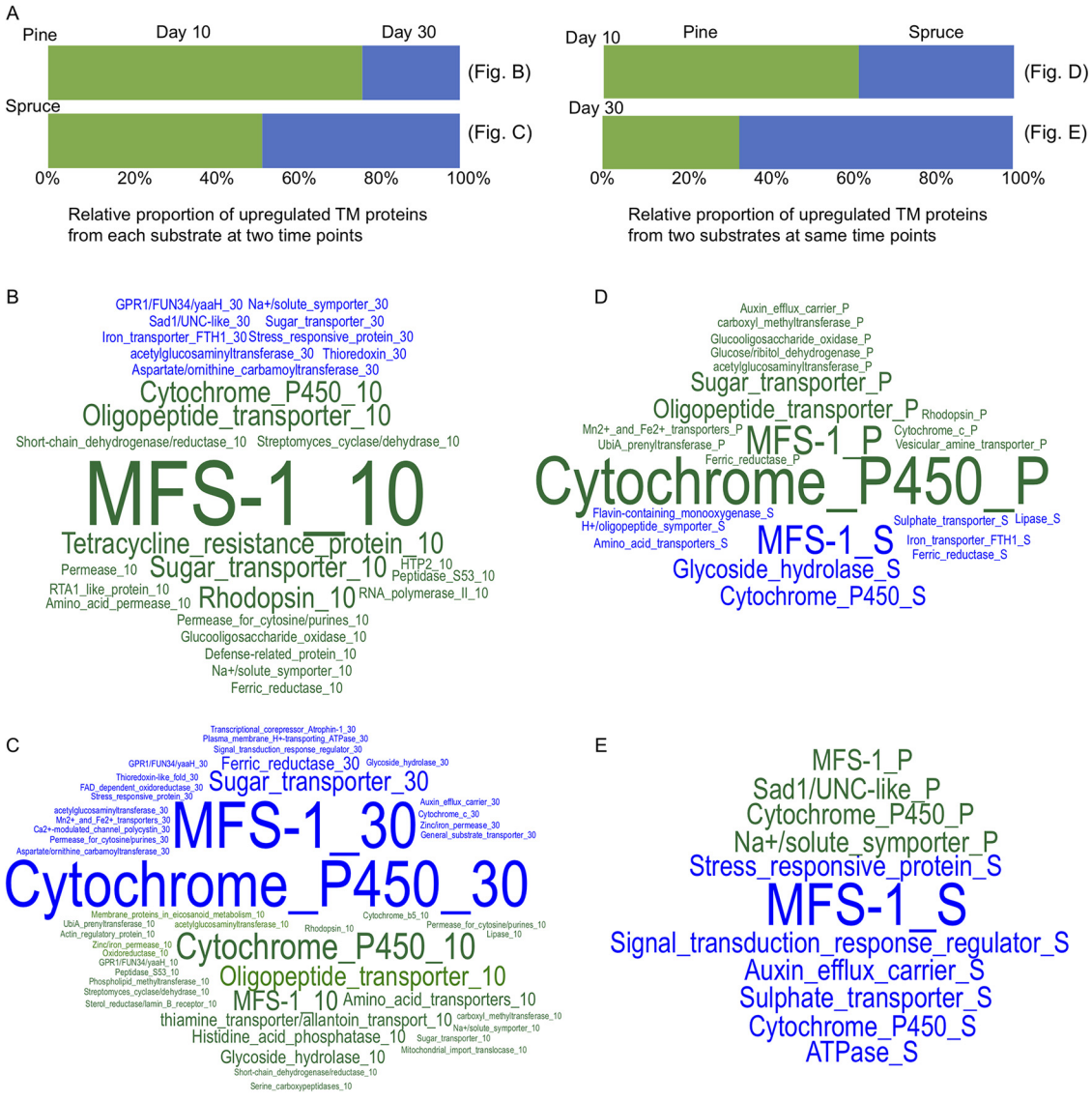

FIG 4 Annotations of DEGs on wood wafers having TM domains. (A) Distribution in relative proportion of TM proteins at different time points (left) and on different substrates (right). For each category, only the upregulated gene at one time point/on one substrate relative to the other time point/substrate was considered. (B to E) showing the details for stacked bars in the panel A. The font size in the word cloud is directly related to the word (protein) frequency in each panel. The colors of words are consistent with the conditions used in panel A.

of substrate (see Fig. S4 and S5). Samples on submerged culture at day 5 were more similar to samples from wood wafers at day 30, than wood wafer samples at day 10 (Mann-Whitney U test, $P < 0.00001$) (see Fig. S4). A neighbor-joining analysis of samples further indicated that the samples at day 5 were more distant from samples at day 10 than at day 30 (Fig. 5).

DISCUSSION

***Fomitopsis pinicola* exhibits substrate-dependent and time-dependent differential gene expression.** *Fomitopsis pinicola* produces similar sets of wood-degrading enzymes on both hardwood and softwood substrates, as do other wood decay fungi (47, 50). Nevertheless, there are differences in the expression of specific genes, yielding substrate-specific expression profiles (Fig. 1; see also Table S1). Genome and transcriptome analyses of other brown rot species have suggested that they employ nonenzymatic Fenton chemistry to generate hydroxyl radicals, which are generated by various redox systems (49, 50, 69, 70). In this study, differentially expressed decay-related oxidoreductases included laccase, AA3 (aryl alcohol oxidase), benzoquinone reductase, Fe(III)-reducing glycopeptides

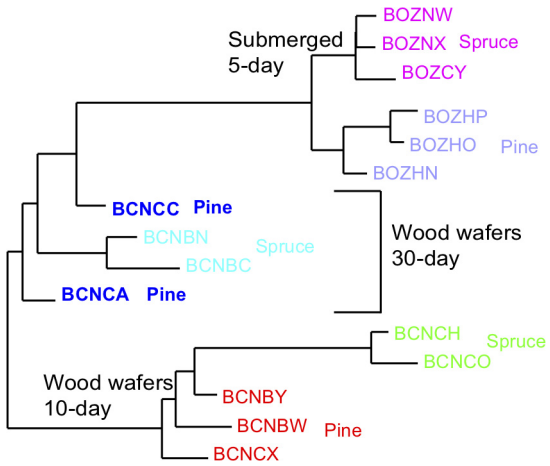

FIG 5 Cross-culture method comparisons. A neighbor-joining tree with branch lengths inferred using (1 – Spearman's rho) for all pairs of gene expression profiles is shown.

(GLP), and oxalate oxidase/decarboxylases (OXO) (Fig. 1 and 3C and D; see also Table S3). Glycoside hydrolases are also important for brown-rot decay, and we found 16 kinds of upregulated GHs (GH1, GH3, GH5, GH16, GH17, GH18, GH28, GH30, GH31, GH43, GH45, GH78, GH79, GH92, and GH128) from different substrates and time points (Fig. 1 and 3C and D; see also Table S3). The biological roles of some GHs are uncertain. For example, GH18 and GH16 are related to lysis of fungal mycelium, but recent studies in white-rot fungi show that the two gene families are differentially expressed during wood decay (49, 71), suggesting potential roles in wood decay. In particular, GH16 enzymes may attack β-1,3-glucans or xyloglucans, which play significant roles in hemicellulose degradation (72, 73). Along the time course on wood wafers, upregulated CAZymes are greater at day 10 than at day 30, whereas upregulated AA enzymes are greater at day 30 than at day 10 (Fig. 3C and D). This is not consistent with recent observations in *P. placenta* (17), where greater numbers of upregulated redox enzymes occurred at early stages of decay. A recent study suggests that lignocellulose oxidation by *F. pinicola* fluctuates for 3 months in submerged culture supplemented with spruce wood (74).

Unknown "hypothetical" proteins also contribute to substrate-specific responses. For instance, 50% (146) of the DEGs (294) between pine and spruce after a 10-day incubation lack clear annotations according to InterPro prediction. Among these, 44 proteins (30%) were predicted to have secretion signals, and 47 (32%) have TM domains, suggesting that they may contribute to extracellular processes, including plant cell wall decomposition, or transport of solutes across fungal cell membranes (74).

Pine and spruce "softwood" substrates elicit distinct gene expression profiles. Transcriptomes from 5-day-old submerged cultures showed that global gene expression profiles on pine were more similar to those from aspen than those from spruce (Fig. 1; see also Fig. S1). This was surprising, because pine and spruce are both softwoods in the Pinaceae, whereas aspen is a hardwood. These findings suggest that it may be misleading to generalize from gene expression results on individual wood species to all "softwoods" (gymnosperms) or "hardwoods" (angiosperms). Moreover, prior studies using different genotypes of aspen (49, 60) or different wood types from pine and spruce (i.e., heartwood, sapwood, and tension wood [55]) demonstrate that gene expression may vary according to the genotype of the host species, or the specific kind of wood that is used. Subtle differences in wood anatomy, physical properties and/or chemical composition may substantially impact transcript profiles. Thus, to maximize comparability among studies it will be necessary not only to select a uniform set of species (perhaps focusing on plants with the greatest potential as feedstocks for biofuel production) but also to consider genetic diversity within species and the anatomical and chemical properties of wood samples.

Large differences exist in wood components for pine and spruce versus aspen. Lignin content is higher (27 to 30%) compared to aspen (22%), while cellulose and hemicellulose are approximately the same. However, the hemicellulose composition is largely acetylated glucuronoxylans in hardwoods and acetylated galactoglucomannans in softwoods (24, 75). Other relatively minor wood components, such as extractives, may have a greater impact on specific gene expression as shown for the white rot fungus *Phlebiopsis gigantea* (76).

Brown rot Polyporales have elevated expression of certain P450s on pine versus aspen substrates. *Fomitopsis pinicola* is the third brown rot species in the Antrodia clade of the Polyporales to be used for comparative transcriptomic analyses on different wood substrates. Vanden Wymelenberg et al. (56) and Gaskell et al. (50) analyzed *W. cocos* and *P. placenta*, respectively, and both studies compared aspen and pine substrates in submerged cultures sampled at 5 days, as in the present study. Under these conditions, in all three studies there were few genes upregulated (>4-fold, false discovery rate [FDR] < 0.05) on pine versus aspen, including 19 genes in *P. placenta*, 5 genes in *W. cocos*, and 12 genes in *F. pinicola* (Fig. 1; see also Table S1). In each species, the upregulated transcripts on pine include genes encoding cytochrome P450s (10 in *P. placenta*, 3 in *W. cocos*, and 1 in *F. pinicola*), suggesting that these may contribute to a common response to pine relative to aspen. The precise function of these P450s remains to be established, but depletion of small lignin derivatives or extractive compounds observed with ToF-SIMS is consistent with a role for these enzymes in metabolism of toxic breakdown products (see the supplemental material).

Culture methods greatly affect gene expression. Transcriptomic studies of wood decay in fungi usually employ submerged culture methods (29, 47, 50, 64, 77), wood wafers (49) or sawdust (54, 55). Of these methods, solid wafers may best mimic "natural" conditions in which the porosity of sound wood excludes many enzymes during incipient decay (78, 79). However, steam sterilization likely impacts substrate accessibility, and this pretreatment is no doubt more pronounced when the substrate is ground and dispersed as in submerged cultures.

Global analysis of gene expression profiles on pine and spruce in submerged cultures at 5 days or wood wafers sampled at 10 and 30 days indicates that culture conditions have a greater impact on overall transcriptome profiles than substrate species, and the global gene expression pattern at day 5 in submerged substrates is more similar to that on wood wafers at day 30 than on wood wafers at day 10 (see Fig. S4). The number of DEGs reflects the sensitivity of *F. pinicola* in recognizing substrates. Among the three sampling points, *F. pinicola* at day 5 in submerged culture has the fewest DEGs. Thus, *F. pinicola* in submerged culture exhibits the least sensitivity to substrates among the conditions that we employed. It is not clear whether this effect is a consequence of the time of sampling or the culture conditions. Additional studies with overlapping time points in both submerged cultures and wood wafers could help discriminate the relative effects of time of sampling versus culture conditions.

Conclusions. *Fomitopsis pinicola*, a wood-decaying Agaricomycete with a broad range of softwood and hardwood hosts, exhibits differential gene expression on different wood substrates (aspen, pine, and spruce) and under different culture conditions (submerged substrates versus wood wafers). Many of the DEGs identified here encode enzymes with known or predicted functions in plant cell wall decomposition, suggesting that *F. pinicola* can modulate its decay apparatus according to substrate. However, culture conditions (submerged ground wood versus wood wafers) and sampling times had a greater impact on overall gene expression profiles than did wood species, which highlights the need for standardization of experimental parameters in studies of wood decay mechanisms. Comparisons of gene expression on pine versus aspen in 5-day-old submerged cultures of *F. pinicola*, *P. placenta* and *W. cocos*, which are all brown rot species of the Antrodia clade (Polyporales), indicate that genes encoding some cytochrome P450s may be upregulated on pine. To assess the generality of these results, it will be necessary to study gene expression in additional species (ideally represented by multiple strains) of brown rot Polyporales on aspen, pine and spruce substrates.

MATERIALS AND METHODS

Culture conditions. *Fomitopsis pinicola* FP-58527 was obtained from the Forest Mycology Center, USDA Forest Products Laboratory (Madison, WI). Originally isolated from *Pinus ponderosa*, a draft genome sequence of this strain was analyzed by Floudas et al. (9), and the version 3 assembly is publicly available through the JGI portal (https://genome.jgi.doe.gov/Fompi3/Fompi3.home.html). Two culture methods were used to explore the transcriptome of *F. pinicola* on different substrates. Two-liter flasks containing 250 ml of basal salt media were supplemented with wood ground in Wiley-mill with a #10 mesh screen. Each flask contained wood of quaking aspen (*Populus tremuloides*), loblolly pine (*Pinus taeda*), or white spruce (*Picea glauca*) as the sole carbon source. The basal medium was prepared as described previously (50). Following autoclaving at 121°C for 15 min, triplicate cultures for each substrate were inoculated with mycelium scraped from malt extract agar (2% [wt/wt] malt extract, 2% [wt/wt] glucose, 0.5% peptone, 1.5% agar) and placed on a rotary shaker (150 rpm) at 22 to 24°C. Five days after inoculation, mycelia and pellets of various sizes were collected by filtration through Miracloth (Calbiochem) and stored at −80°C. In addition to submerged cultures, the mycelium was also cultured on wood wafers of the same three species in solid-block jar microcosms for solid-state culturing. Wood wafers were created from the same individual wood samples that were used to obtain milled substrates used in submerged cultures. The soil mixture for the microcosm was prepared using two parts of loam soil, two parts of vermiculite, and one part of peat moss that was wetted to capacity and placed in glass jars (473 ml). Two wood feeder strips corresponding to each type of wood were placed together on the top of the soil mixture and autoclaved twice for 1 h at 121°C with a 24-h period in between sterilizations. A 5-mm-diameter plug of media containing mycelium was placed at the corner of the feeder strips. When the mycelium covered the feeder strips completely, thin ($10 \times 15 \times 1$ mm), longitudinally cut wood wafers of each type of wood were placed on the feeder strips and incubated at 22°C. The wood wafers were removed after 10 and 30 days snap-frozen in liquid nitrogen and stored at −80°C. There were three replicates for each treatment.

RNA extraction and RNA-seq library construction. Prior to extraction, colonized ground wood and wafer samples were pulverized under liquid nitrogen in a SPEX 6775 mill (Metuchen, NJ). A modified version of the method of Miyauchi et al. (80) was used for RNA purification from the SPEX-milled wafer. The samples were transferred to Oak Ridge tubes containing 12 ml of TRIzol. To disperse the material, the tubes were vortexed, and the contents were drawn three to five times into a polypropylene pipette. Chloroform (2.4 ml) was added with a glass pipette, and the suspension was briefly vortexed. After standing for 2 to 3 min, the tubes were centrifuged in the prechilled JA-17 rotor at $40,000 \times g$ for 15 min at 4°C. With minimal disturbance to the interface, the aqueous phase (6 ml) was transferred to a new Oak Ridge tube, and 0.6 volumes (3.6 ml) of isopropyl alcohol were added. The contents were gently mixed by inverting several times, and then the tubes were incubated at −20°C for 1 to 2 h. The nucleic acids were pelleted by centrifugation at $40,000 \times g$ for 10 min at 4°C. After careful decanting, the pellet was washed twice with 75% ethanol and air dried. The RNA was resuspended in 887.5 μl of diethyl pyrocarbonate (DEPC)-treated water and transferred to a sterile Eppendorf tube. The sample was DNase treated with Qiagen's RNase-free DNase set by adding 100 μl of RDD buffer and 12.5 μl of DNase (3 U/μl). After 20 min, another 3 U of DNase was added. RNA was precipitated by adding 330 μl of 8 M LiCl, followed by incubation at −20°C for at least 1 h. The Eppendorf tubes were then centrifuged in prechilled JA-18.1 at 12,000 rpm ($\sim 18,000 \times g$) for 20 min, and the pellet was resuspended in 150 μl of isopropyl alcohol. The samples were then centrifuged in JA-18.1 at $12,000 \times g$ for 5 min and washed twice with 1 ml of 70% ethanol. Droplets of remaining ethanol were aspirated to hasten air drying. The dry pellet was resuspended in 25 μl of DEPC-water and placed at 55°C for 5 min to dissolve. All RNA samples were quantified by a Qubit fluorometer (Thermo Fisher Scientific) and quality checked with a 2100 BioAnalyzer (Agilent), respectively.

Plate-based RNA sample prep was performed on the Perkin-Elmer Sciclone NGS robotic liquid handling system using the Illumina TruSeq Stranded mRNA HT sample prep kit utilizing poly(A) selection of mRNA according to the protocol outlined by Illumina in their user guide and using the following conditions: total RNA starting material was 1 μg per sample, and eight cycles of PCR were used for library amplification. The prepared libraries were quantified using KAPA Biosystem's next-generation sequencing library qPCR kit and run on a Roche LightCycler 480 real-time PCR instrument. The quantified libraries were then multiplexed and prepared for sequencing on the Illumina HiSeq sequencing platform utilizing a TruSeq Rapid paired-end cluster kit, v4. Sequencing of the flow cell was performed on the Illumina HiSeq2000 sequencer using HiSeq TruSeq SBS sequencing kits, v4, following a 1×101 indexed run recipe.

Identification of differentially expressed genes. Raw reads were filtered and trimmed using the JGI QC pipeline. Using BBDuk (https://sourceforge.net/projects/bbmap/), raw reads were evaluated for sequence artifacts by kmer matching (kmer = 25), allowing one mismatch, and any detected artifact was trimmed from the 3′ end of the reads. RNA spike-in reads, PhiX reads and reads containing any Ns were removed. Quality trimming was performed using the phred trimming method set at Q6. Finally, following trimming, reads under the length 25 nucleotides were removed. Filtered reads from each library were aligned to the haploid *F. pinicola* FP-58527 genome using HISAT (81) (see Table S5). featureCounts (82) was used to generate the raw gene counts using gff3 annotations (https://genome.jgi.doe.gov/Fompi3/Fompi3.info.html). Only primary hits assigned to the reverse strand were included in the raw gene counts (-s 2 -p –primary options). FPKM normalized gene counts were calculated by Cufflinks (83). edgeR (84) was subsequently used to determine which genes were differentially expressed between pairs of conditions. The parameters used to call a DEG between conditions were a P value of <0.05 and a $\log_2$-fold change of ≥ 4. SignalP 4.1 (85) was used to search for secretory signal peptides in DEGs proteins. TMHMM 2.0 (86) was used to predict and characterize TM domains in proteins encoded by DEGs, with default parameters. Functional categories enriched with DEGs were identified using FungiFun2 with an FDR of <0.05 (87).

Data availability. Transcriptome data set have been deposited in the NCBI Sequence Read Archive, accession numbers SRP140951 to SRP140968 (see Table S4 for details).

SUPPLEMENTAL MATERIAL

Supplemental material is available online only.

SUPPLEMENTAL FILE 1, PDF file, 0.5 MB.

SUPPLEMENTAL FILE 2, XLSX file, 2 MB.

SUPPLEMENTAL FILE 3, XLSX file, 2.4 MB.

SUPPLEMENTAL FILE 4, XLSX file, 0.01 MB.

SUPPLEMENTAL FILE 5, XLSX file, 0.01 MB.

ACKNOWLEDGMENTS

This study was supported by National Science Foundation awards IOS-1456777 (to D.S.H.), IOS-1456548 (to R.A.B.), IOS-1456958 (to I.V.G.), and DEB-1457721 (to D.C.).

REFERENCES

1. Gilbertson RL. 1980. Wood-rotting fungi of North America. Mycologia 72:1–49. https://doi.org/10.2307/3759417.
2. Nilsson T, Daniel G, Kirk TK, Obst JR. 1989. Chemistry and microscopy of wood decay by some higher ascomycetes. Holzforschung 43:11–18. https://doi.org/10.1515/hfsg.1989.43.1.11.
3. Shary S, Ralph SA, Hammel KE. 2007. New insights into the ligninolytic capability of a wood decay ascomycete. Appl Environ Microbiol 73:6691–6694. https://doi.org/10.1128/AEM.01361-07.
4. Baldrian P, Valaskova V. 2008. Degradation of cellulose by basidiomycetous fungi. FEMS Microbiol Rev 32:501–521. https://doi.org/10.1111/j.1574-6976.2008.00106.x.
5. Lundell TK, Makela MR, Hilden K. 2010. Lignin-modifying enzymes in filamentous basidiomycetes–ecological, functional and phylogenetic review. J Basic Microbiol 50:5–20. https://doi.org/10.1002/jobm.200900338.
6. Eriksson KE, Blanchette RA, Ander P. 1990. Microbial and enzymatic degradation of wood and wood components. Springer, Berlin, Germany.
7. Blanchette RA. 1995. Degradation of the lignocellulose complex in wood. Can J Bot 73:999–1010. https://doi.org/10.1139/b95-350.
8. Worrall JJ, Anagnost SE, Zabel RA. 1997. Comparison of wood decay among diverse lignicolous fungi. Mycologia 89:199–219. https://doi.org/10.2307/3761073.
9. Floudas D, Binder M, Riley R, Barry K, Blanchette RA, Henrissat B, Martínez AT, Otillar R, Spatafora JW, Yadav JS, Aerts A, Benoit I, Boyd A, Carlson A, Copeland A, Coutinho PM, de Vries RP, Ferreira P, Findley K, Foster B, Gaskell J, Glotzer D, Górecki P, Heitman J, Hesse C, Hori C, Igarashi K, Jurgens JA, Kallen N, Kersten P, Kohler A, Kües U, Kumar TKA, Kuo A, LaButti K, Larrondo LF, Lindquist E, Ling A, Lombard V, Lucas S, Lundell T, Martin R, McLaughlin DJ, Morgenstern I, Morin E, Murat C, Nagy LG, Nolan M, Ohm RA, Patyshakuliyeva A, et al. 2012. The Paleozoic origin of enzymatic lignin decomposition reconstructed from 31 fungal genomes. Science 336:1715–1719. https://doi.org/10.1126/science.1221748.
10. Nagy LG, Riley R, Tritt A, Adam C, Daum C, Floudas D, Sun H, Yadav JS, Pangilinan J, Larsson KH, Matsuura K, Barry K, Labutti K, Kuo R, Ohm RA, Bhattacharya SS, Shirouzu T, Yoshinaga Y, Martin FM, Grigoriev IV, Hibbett DS. 2016. Comparative genomics of early-diverging mushroom-forming fungi provides Insights into the origins of lignocellulose decay capabilities. Mol Biol Evol 33:959–970. https://doi.org/10.1093/molbev/msv337.
11. Riley R, Salamov AA, Brown DW, Nagy LG, Floudas D, Held BW, Levasseur A, Lombard V, Morin E, Otillar R, Lindquist EA, Sun H, LaButti KM, Schmutz J, Jabbour D, Luo H, Baker SE, Pisabarro AG, Walton JD, Blanchette RA, Henrissat B, Martin F, Cullen D, Hibbett DS, Grigoriev IV. 2014. Extensive sampling of basidiomycete genomes demonstrates inadequacy of the white-rot/brown-rot paradigm for wood decay fungi. Proc Natl Acad Sci U S A 111:9923–9928. https://doi.org/10.1073/pnas.1400592111.
12. Cowling EB. 1961. Comparative biochemistry of the decay of sweetgum sapwood by white-rot and brown-rot fungi. U.S. Department of Agriculture, Washington, DC.
13. Kleman-Leyer K. 1994. Depolymerization of cellulose by brown rot fungi: comparison to that by cellulolytic systems of two non-wood degrading microorganisms. University of Wisconsin, Madison, WI.
14. Brischke C, Welzbacher CR, Huckfeldt T. 2008. Influence of fungal decay by different basidiomycetes on the structural integrity of Norway Spruce wood. Holz Roh Werkst 66:433–438. https://doi.org/10.1007/s00107-008-0257-1.
15. Yelle DJ, Ralph J, Lu F, Hammel KE. 2008. Evidence for cleavage of lignin by a brown rot basidiomycete. Environ Microbiol 10:1844–1849. https://doi.org/10.1111/j.1462-2920.2008.01605.x.
16. Yelle DJ, Wei D, Ralph J, Hammel KE. 2011. Multidimensional NMR analysis reveals truncated lignin structures in wood decayed by the brown rot basidiomycete *Postia placenta*. Environ Microbiol 13:1091–1100. https://doi.org/10.1111/j.1462-2920.2010.02417.x.
17. Zhang J, Presley GN, Hammel KE, Ryu JS, Menke JR, Figueroa M, Hu D, Orr G, Schilling JS. 2016. Localizing gene regulation reveals a staggered wood decay mechanism for the brown rot fungus *Postia placenta*. Proc Natl Acad Sci U S A 113:10968–10973. https://doi.org/10.1073/pnas.1608454113.
18. Gilbertson RL, Ryvarden L. 1986. North American polypores. Oslo Fungiflora 1:1–443.
19. Gilbertson RL, Ryvarden L. 1987. North American polypores. Oslo Fungiflora 2:1–885.
20. Ginns J, Lefebvre MNL. 1993. Lignicolous corticioid fungi (Basidiomycota) of North America: systematics, distribution, and ecology. Mycologia Memoir 19:1–247. American Phytopathological Society Press, Saint Paul, MN.
21. Gilbertson RL. 1981. North American wood-rotting fungi that cause brown rots. Mycotaxon 12:372–416.
22. Hibbett DS, Donoghue MJ. 2001. Analysis of character correlations among wood decay mechanisms, mating systems, and substrate ranges in homobasidiomycetes. Syst Biol 50:215–242. https://doi.org/10.1080/10635150151125879.
23. Ek M, Gellerstedt G, Henriksson G. 2009. Wood chemistry and wood biotechnology. Walter De Gruyter, Inc, Berlin, Germany.
24. Fengel D, Wegener G. 1989. Wood: chemistry, ultrastructure, reactions. Walter De Gruyter, Inc, Berlin, Germany.
25. Timell TE. 1967. Recent progress in the chemistry of wood hemicelluloses. Wood Scitechnol 1:45–70. https://doi.org/10.1007/BF00592255.
26. Cohen R, Jensen KA, Houtman CJ, Hammel KE. 2002. Significant levels of extracellular reactive oxygen species produced by brown rot basidiomycetes on cellulose. FEBS Lett 531:483–488. https://doi.org/10.1016/s0014-5793(02)03589-5.
27. Xu G, Goodell B. 2001. Mechanisms of wood degradation by brown-rot fungi: chelator-mediated cellulose degradation and binding of iron by cellulose. J Biotechnol 87:43–57. https://doi.org/10.1016/s0168-1656(00)00430-2.
28. Goodell B. 2003. Brown rot fungal degradation of wood: our evolving view, p 97–118. *In* Goodell B, Nicholas D, Schultz T (ed), Wood deterioration and preservation. American Chemical Society, Washington, DC.
29. Martinez D, Challacombe J, Morgenstern I, Hibbett D, Schmoll M, Kubicek CP, Ferreira P, Ruiz-Duenas FJ, Martinez AT, Kersten P, Hammel KE, Vanden Wymelenberg A, Gaskell J, Lindquist E, Sabat G, Bondurant SS, Larrondo LF, Canessa P, Vicuna R, Yadav J, Doddapaneni H, Subramanian V, Pisabarro AG, Lavín JL, Oguiza JA, Master E, Henrissat B, Coutinho PM, Harris P, Magnuson JK, Baker SE, Bruno K, Kenealy W, Hoegger PJ, Kües U, Ramaiya P, Lucas S, Salamov A, Shapiro H, Tu H, Chee CL, Misra M, Xie G, Teter S, Yaver D, James T, Mokrejs M, Pospisek M, Grigoriev IV, Brettin T, et al. 2009. Genome, transcriptome, and secretome analysis of wood decay fungus *Postia placenta* supports unique mechanisms of lignocellulose conversion. Proc Natl Acad Sci U S A 106:1954–1959. https://doi.org/10.1073/pnas.0809575106.
30. Hirano T, Tanaka H, Enoki A. 1997. Relationship between production of hydroxyl radicals and degradation of wood by the brown-rot fungus,

Tyromyces palustris. Holzforshung 51:389–395. https://doi.org/10.1515/hfsg.1997.51.5.389.
31. Tanaka H, Itakura S, Enoke A. 1999. Hydroxyl radical generation by an extracellular low-molecular weight substance and phenol oxidase activity during wood degradation by the white-rot basidiomycete *Phanerochaete chrysosporium*. Holzforschung 53:21–28. https://doi.org/10.1515/HF.1999.004.
32. Hirano T, Enoki A, Tanaka H. 2000. Immunogold labeling of an extracellular substance producing hydroxyl radicals in wood degraded by brown-rot fungus *Tyromyces palustris*. J Wood Sci 46:45–51. https://doi.org/10.1007/BF00779552.
33. Tanaka H, Yoshida G, Baba Y, Matsumura K, Wasada H, Murata J, Agawa M, Itakura S, Enoki A. 2007. Characterization of a hydroxyl-radical-producing glycoprotein and its presumptive genes from the white-rot basidiomycete *Phanerochaete chrysosporium*. J Biotechnol 128:500–511. https://doi.org/10.1016/j.jbiotec.2006.12.010.
34. Shimokawa T, Nakamura M, Hayashi N, Ishihara M. 2004. Production of 2,5-dimethoxyhydroquinone by the brown-rot fungus *Serpuyla lacrymans* to drive extracellular Fenton reaction. Holzforschung 58:305–310. https://doi.org/10.1515/HF.2004.047.
35. Suzuki MR, Hunt CG, Houtman CJ, Dalebroux ZD, Hammel KE. 2006. Fungal hydroquinones contribute to brown rot of wood. Environ Microbiol 8:2214–2223. https://doi.org/10.1111/j.1462-2920.2006.01160.x.
36. Varela E, Tien M. 2003. Effect of pH and oxalate on hydroquinone-derived hydroxyl radical formation during brown rot wood degradation. Appl Environ Microbiol 69:6025–6031. https://doi.org/10.1128/AEM.69.10.6025-6031.2003.
37. Kaneko S, Yoshitake K, Itakura S, Tanaka H, Enoki A. 2005. Relationship between production of hydroxyl radicals and degradation of wood, crystalline cellulose, and lignin-related compound or accumulation of oxalic acid in cultures of brown-rot fungi. J Wood Sci 51:262–269. https://doi.org/10.1007/s10086-004-0641-3.
38. Jensen KA, Jr, Houtman CJ, Ryan ZC, Hammel KE. 2001. Pathways for extracellular Fenton chemistry in the brown rot basidiomycete *Gloeophyllum trabeum*. Appl Environ Microbiol 67:2705–2711. https://doi.org/10.1128/AEM.67.6.2705-2711.2001.
39. Wei D, Houtman CJ, Kapich AN, Hunt CG, Cullen D, Hammel KE. 2010. Laccase and its role in production of extracellular reactive oxygen species during wood decay by the brown rot basidiomycete *Postia placenta*. Appl Environ Microbiol 76:2091–2097. https://doi.org/10.1128/AEM.02929-09.
40. Kersten P, Cullen D. 2007. Extracellular oxidative systems of the lignin-degrading basidiomycete *Phanerochaete chrysosporium*. Fungal Genet Biol 44:77–87. https://doi.org/10.1016/j.fgb.2006.07.007.
41. Hammel KE, Cullen D. 2008. Role of fungal peroxidases in biological ligninolysis. Curr Opin Plant Biol 11:349–355. https://doi.org/10.1016/j.pbi.2008.02.003.
42. Benz JP, Chau BH, Zheng D, Bauer S, Glass NL, Somerville CR. 2014. A comparative systems analysis of polysaccharide-elicited responses in *Neurospora crassa* reveals carbon source-specific cellular adaptations. Mol Microbiol 91:275–299. https://doi.org/10.1111/mmi.12459.
43. Couturier M, Navarro D, Chevret D, Henrissat B, Piumi F, Ruiz-Duenas FJ, Martinez AT, Grigoriev IV, Riley R, Lipzen A, Berrin JG, Master ER, Rosso MN. 2015. Enhanced degradation of softwood versus hardwood by the white-rot fungus *Pycnoporus coccineus*. Biotechnol Biofuels 8:216. https://doi.org/10.1186/s13068-015-0407-8.
44. Sato S, Liu F, Koc H, Tien M. 2007. Expression analysis of extracellular proteins from *Phanerochaete chrysosporium* grown on different liquid and solid substrates. Microbiology (Reading) 153:3023–3033. https://doi.org/10.1099/mic.0.2006/000513-0.
45. Ravalason H, Jan G, Molle D, Pasco M, Coutinho PM, Lapierre C, Pollet B, Bertaud F, Petit-Conil M, Grisel S, Sigoillot JC, Asther M, Herpoel-Gimbert I. 2008. Secretome analysis of *Phanerochaete chrysosporium* strain CIRM-BRFM41 grown on softwood. Appl Microbiol Biotechnol 80:719–733. https://doi.org/10.1007/s00253-008-1596-x.
46. Mahajan S, Master ER. 2010. Proteomic characterization of lignocellulose-degrading enzymes secreted by *Phanerochaete carnosa* grown on spruce and microcrystalline cellulose. Appl Microbiol Biotechnol 86:1903–1914. https://doi.org/10.1007/s00253-010-2516-4.
47. Vanden Wymelenberg A, Gaskell J, Mozuch M, Sabat G, Ralph J, Skyba O, Mansfield SD, Blanchette RA, Martinez D, Grigoriev I, Kersten PJ, Cullen D. 2010. Comparative transcriptome and secretome analysis of wood decay fungi *Postia placenta* and *Phanerochaete chrysosporium*. Appl Environ Microbiol 76:3599–3610. https://doi.org/10.1128/AEM.00058-10.
48. Mattila HK, Makinen M, Lundell T. 2020. Hypoxia is regulating enzymatic wood decomposition and intracellular carbohydrate metabolism in filamentous white rot fungus. Biotechnol Biofuels 13:26. https://doi.org/10.1186/s13068-020-01677-0.
49. Skyba O, Cullen D, Douglas CJ, Mansfield SD. 2016. Gene expression patterns of wood decay fungi *Postia placenta* and *Phanerochaete chrysosporium* are influenced by wood substrate composition during degradation. Appl Environ Microbiol 82:4387–4400. https://doi.org/10.1128/AEM.00134-16.
50. Gaskell J, Blanchette RA, Stewart PE, BonDurant SS, Adams M, Sabat G, Kersten P, Cullen D. 2016. Transcriptome and secretome analyses of the wood decay fungus *Wolfiporia cocos* support alternative mechanisms of lignocellulose conversion. Appl Environ Microbiol 82:3979–3987. https://doi.org/10.1128/AEM.00639-16.
51. MacDonald J, Doering M, Canam T, Gong Y, Guttman DS, Campbell MM, Master ER. 2011. Transcriptomic responses of the softwood-degrading white-rot fungus *Phanerochaete carnosa* during growth on coniferous and deciduous wood. Appl Environ Microbiol 77:3211–3218. https://doi.org/10.1128/AEM.02490-10.
52. Macdonald J, Master ER. 2012. Time-dependent profiles of transcripts encoding lignocellulose-modifying enzymes of the white rot fungus *Phanerochaete carnosa* grown on multiple wood substrates. Appl Environ Microbiol 78:1596–1600. https://doi.org/10.1128/AEM.06511-11.
53. Rytioja J, Hilden K, Di Falco M, Zhou M, Aguilar-Pontes MV, Sietio OM, Tsang A, de Vries RP, Makela MR. 2017. The molecular response of the white-rot fungus *Dichomitus squalens* to wood and non-woody biomass as examined by transcriptome and exoproteome analyses. Environ Microbiol 19:1237–1250. https://doi.org/10.1111/1462-2920.13652.
54. Suzuki H, MacDonald J, Syed K, Salamov A, Hori C, Aerts A, Henrissat B, Wiebenga A, VanKuyk PA, Barry K, Lindquist E, LaButti K, Lapidus A, Lucas S, Coutinho P, Gong Y, Samejima M, Mahadevan R, Abou-Zaid M, de Vries RP, Igarashi K, Yadav JS, Grigoriev IV, Master ER. 2012. Comparative genomics of the white-rot fungi, *Phanerochaete carnosa* and *P chrysosporium*, to elucidate the genetic basis of the distinct wood types they colonize. BMC Genomics 13:444. https://doi.org/10.1186/1471-2164-13-444.
55. Yakovlev I, Vaaje-Kolstad G, Hietala AM, Stefańczyk E, Solheim H, Fossdal CG. 2012. Substrate-specific transcription of the enigmatic GH61 family of the pathogenic white-rot fungus *Heterobasidion irregulare* during growth on lignocellulose. Appl Microbiol Biotechnol 95:979–990. https://doi.org/10.1007/s00253-012-4206-x.
56. Vanden Wymelenberg A, Gaskell J, Mozuch M, BonDurant SS, Sabat G, Ralph J, Skyba O, Mansfield SD, Blanchette RA, Grigoriev IV, Kersten PJ, Cullen D. 2011. Significant alteration of gene expression in wood decay fungi *Postia placenta* and *Phanerochaete chrysosporium* by plant species. Appl Environ Microbiol 77:4499–4507. https://doi.org/10.1128/AEM.00508-11.
57. Yakovlev IA, Hietala AM, Courty PE, Lundell T, Solheim H, Fossdal CG. 2013. Genes associated with lignin degradation in the polyphagous white-rot pathogen *Heterobasidion irregulare* show substrate-specific regulation. Fungal Genet Biol 56:17–24. https://doi.org/10.1016/j.fgb.2013.04.011.
58. Doddapaneni H, Chakraborty R, Yadav JS. 2005. Genome-wide structural and evolutionary analysis of the P450 monooxygenase genes (P450ome) in the white rot fungus *Phanerochaete chrysosporium*: evidence for gene duplications and extensive gene clustering. BMC Genomics 6:92. https://doi.org/10.1186/1471-2164-6-92.
59. Doddapaneni H, Yadav JS. 2005. Microarray-based global differential expression profiling of P450 monooxygenases and regulatory proteins for signal transduction pathways in the white rot fungus *Phanerochaete chrysosporium*. Mol Genet Genomics 274:454–466. https://doi.org/10.1007/s00438-005-0051-2.
60. Gaskell J, Marty A, Mozuch M, Kersten PJ, Splinter BonDurant S, Sabat G, Azarpira A, Ralph J, Skyba O, Mansfield SD, Blanchette RA, Cullen D. 2014. Influence of *Populus* genotype on gene expression by the wood decay fungus *Phanerochaete chrysosporium*. Appl Environ Microbiol 80:5828–5835. https://doi.org/10.1128/AEM.01604-14.
61. Farr DF, Rossman AY. 2018. Fungal databases, U.S. national fungus collections. ARS/USDA, Washington, DC. https://nt.arsgrin.gov/fungaldatabases/. Accessed 16 January 2018.
62. Vanden Wymelenberg A, Sabat G, Martinez D, Rajangam AS, Teeri TT, Gaskell J, Kersten PJ, Cullen D. 2005. The *Phanerochaete chrysosporium* secretome: database predictions and initial mass spectrometry peptide identifications in cellulose-grown medium. J Biotechnol 118:17–34. https://doi.org/10.1016/j.jbiotec.2005.03.010.
63. Vanden Wymelenberg A, Minges P, Sabat G, Martinez D, Aerts A, Salamov A, Grigoriev I, Shapiro H, Putnam N, Belinky P, Dosoretz C, Gaskell J, Kersten P, Cullen D. 2006. Computational analysis of the *Phanerochaete*

chrysosporium v2.0 genome database and mass spectrometry identification of peptides in ligninolytic cultures reveals complex mixtures of secreted proteins. Fungal Genet Biol 43:343–356. https://doi.org/10.1016/j.fgb.2006.01.003.
64. Fernandez-Fueyo E, Ruiz-Dueñas FJ, Ferreira P, Floudas D, Hibbett DS, Canessa P, Larrondo LF, James TY, Seelenfreund D, Lobos S, Polanco R, Tello M, Honda Y, Watanabe T, Watanabe T, Ryu JS, San RJ, Kubicek CP, Schmoll M, Gaskell J, Hammel KE, St John FJ, Vanden Wymelenberg A, Sabat G, Splinter BonDurant S, Syed K, Yadav JS, Doddapaneni H, Subramanian V, Lavín JL, Oguiza JA, Perez G, Pisabarro AG, Ramirez L, Santoyo F, Master E, Coutinho PM, Henrissat B, Lombard V, Magnuson JK, Kües U, Hori C, Igarashi K, Samejima M, Held BW, Barry KW, LaButti KM, Lapidus A, Lindquist EA, Lucas SM, et al. 2012. Comparative genomics of *Ceriporiopsis subvermispora* and *Phanerochaete chrysosporium* provide insight into selective ligninolysis. Proc Natl Acad Sci U S A 109:5458–5463. https://doi.org/10.1073/pnas.1119912109.
65. Ryu JS, Shary S, Houtman CJ, Panisko EA, Korripally P, St John FJ, Crooks C, Siika-Aho M, Magnuson JK, Hammel KE. 2011. Proteomic and functional analysis of the cellulase system expressed by *Postia placenta* during brown rot of solid wood. Appl Environ Microbiol 77:7933–7941. https://doi.org/10.1128/AEM.05496-11.
66. Ide M, Ichinose H, Wariishi H. 2012. Molecular identification and functional characterization of cytochrome P450 monooxygenases from the brown-rot basidiomycete *Postia placenta*. Arch Microbiol 194:243–253. https://doi.org/10.1007/s00203-011-0753-2.
67. Syed K, Nelson DR, Riley R, Yadav JS. 2013. Genomewide annotation and comparative genomics of cytochrome P450 monooxygenases (P450s) in the polypore species *Bjerkandera adusta*, *Ganoderma sp*. and *Phlebia brevispora*. Mycologia 105:1445–1455. https://doi.org/10.3852/13-002.
68. Daniel G, Volc J, Filonova L, Plihal O, Kubatova E, Halada P. 2007. Characteristics of *Gloeophyllum trabeum* alcohol oxidase, an extracellular source of H_2O_2 in brown rot decay of wood. Appl Environ Microbiol 73:6241–6253. https://doi.org/10.1128/AEM.00977-07.
69. Klionsky DJ, Abdelmohsen K, Abe A, Abedin MJ, Abeliovich H, Acevedo Arozena A, Adachi H, Adams CM, Adams PD, Adeli K, Adhihetty PJ, Adler SG, Agam G, Agarwal R, Aghi MK, Agnello M, Agostinis P, Aguilar PV, Aguirre-Ghiso J, Airoldi EM, Ait-Si-Ali S, Akematsu T, Akporiaye ET, Al-Rubeai M, Albaiceta GM, Albanese C, Albani D, Albert ML, Aldudo J, Algül H, Alirezaei M, Alloza I, Almasan A, Almonte-Beceril M, Alnemri ES, Alonso C, Altan-Bonnet N, Altieri DC, Alvarez S, Alvarez-Erviti L, Alves S, Amadoro G, Amano A, Amantini C, Ambrosio S, Amelio I, Amer AO, Amessou M, Amon A, An Z, et al. 2016. Guidelines for the use and interpretation of assays for monitoring autophagy, 3rd ed. Autophagy 12:1–222. https://doi.org/10.1080/15548627.2015.1100356.
70. Arantes V, Jellison J, Goodell B. 2012. Peculiarities of brown-rot fungi and biochemical Fenton reaction with regard to their potential as a model for bioprocessing biomass. Appl Microbiol Biotechnol 94:323–338. https://doi.org/10.1007/s00253-012-3954-y.
71. Miyauchi S, Hage H, Drula E, Lesage-Meessen L, Berrin JG, Navarro D, Favel A, Chaduli D, Grisel S, Haon M, Piumi F, Levasseur A, Lomascolo A, Ahrendt S, Barry K, LaButti KM, Chevret D, Daum C, Mariette J, Klopp C, Cullen D, de Vries RP, Gathman AC, Hainaut M, Henrissat B, Hilden KS, Kues U, Lilly W, Lipzen A, Makela MR, Martinez AT, Morel-Rouhier M, Morin E, Pangilinan J, Ram AFJ, Wosten HAB, Ruiz-Duenas FJ, Riley R, Record E, Grigoriev IV, Rosso MN. 2020. Conserved white-rot enzymatic mechanism for wood decay in the *Basidiomycota* genus *Pycnoporus*. DNA Res 27:dsaa011. https://doi.org/10.1093/dnares/dsaa011.
72. Baumann MJ, Eklöf JM, Michel G, Kallas AM, Teeri TT, Czjzek M, Brumer H. 2007. Structural evidence for the evolution of xyloglucanase activity from xyloglucan endo-transglycosylases: biological implications for cell wall metabolism. Plant Cell 19:1947–1963. https://doi.org/10.1105/tpc.107.051391.
73. Nakajima M, Yamashita T, Takahashi M, Nakano Y, Takeda T. 2012. A novel glycosylphosphatidylinositol-anchored glycoside hydrolase from *Ustilago esculenta* functions in β-1,3-glucan degradation. Appl Environ Microbiol 78:5682–5689. https://doi.org/10.1128/AEM.00483-12.
74. Shah F, Mali T, Lundell TK. 2018. Polyporales brown rot species *Fomitopsis pinicola*: enzyme activity profiles, oxalic acid production, and Fe^{3+}-reducing metabolite secretion. Appl Environ Microbiol 84:e02662-17. https://doi.org/10.1128/AEM.02662-17.
75. Sjöström E. 1993. Wood chemistry: fundamentals and applications, 2nd ed. Academic Press, Inc, New York, NY.
76. Hori C, Ishida T, Igarashi K, Samejima M, Suzuki H, Master E, Ferreira P, Ruiz-Duenas FJ, Held B, Canessa P, Larrondo LF, Schmoll M, Druzhinina IS, Kubicek CP, Gaskell JA, Kersten P, St John F, Glasner J, Sabat G, Splinter BonDurant S, Syed K, Yadav J, Mgbeahuruike AC, Kovalchuk A, Asiegbu FO, Lackner G, Hoffmeister D, Rencoret J, Gutierrez A, Sun H, Lindquist E, Barry K, Riley R, Grigoriev IV, Henrissat B, Kues U, Berka RM, Martinez AT, Covert SF, Blanchette RA, Cullen D. 2014. Analysis of the *Phlebiopsis gigantea* genome, transcriptome and secretome provides insight into its pioneer colonization strategies of wood. PLoS Genet 10:e1004759. https://doi.org/10.1371/journal.pgen.1004759.
77. Floudas D, Held BW, Riley R, Nagy LG, Koehler G, Ransdell AS, Younus H, Chow J, Chiniquy J, Lipzen A, Tritt A, Sun H, Haridas S, LaButti K, Ohm RA, Kues U, Blanchette RA, Grigoriev IV, Minto RE, Hibbett DS. 2015. Evolution of novel wood decay mechanisms in Agaricales revealed by the genome sequences of *Fistulina hepatica* and *Cylindrobasidium torrendii*. Fungal Genet Biol 76:78–92. https://doi.org/10.1016/j.fgb.2015.02.002.
78. Blanchette R, Krueger E, Haight J, Akhtar M, Akin D. 1997. Cell wall alterations in loblolly pine wood decayed by the white-rot fungus, *Ceriporiopsis subvermispora*. J Biotechnol 53:203–213. https://doi.org/10.1016/S0168-1656(97)01674-X.
79. Flournoy D, Kirk TK, Highley T. 1991. Wood decay by brown-rot fungi: changes in pore structure and cell wall volume. Holzforschung 45:383–388. https://doi.org/10.1515/hfsg.1991.45.5.383.
80. Miyauchi S, Navarro D, Grisel S, Chevret D, Berrin JG, Rosso MN. 2017. The integrative omics of white-rot fungus *Pycnoporus coccineus* reveals co-regulated CAZymes for orchestrated lignocellulose breakdown. PLoS One 12:e0175528. https://doi.org/10.1371/journal.pone.0175528.
81. Kim D, Langmead B, Salzberg SL. 2015. HISAT: a fast spliced aligner with low memory requirements. Nat Methods 12:357–360. https://doi.org/10.1038/nmeth.3317.
82. Liao Y, Smyth GK, Shi W. 2014. featureCounts: an efficient general purpose program for assigning sequence reads to genomic features. Bioinformatics 30:923–930. https://doi.org/10.1093/bioinformatics/btt656.
83. Trapnell C, Roberts A, Goff L, Pertea G, Kim D, Kelley DR, Pimentel H, Salzberg SL, Rinn JL, Pachter L. 2012. Differential gene and transcript expression analysis of RNA-seq experiments with TopHat and Cufflinks. Nat Protoc 7:562–578. https://doi.org/10.1038/nprot.2012.016.
84. Robinson MD, McCarthy DJ, Smyth GK. 2010. edgeR: a Bioconductor package for differential expression analysis of digital gene expression data. Bioinformatics 26:139–140. https://doi.org/10.1093/bioinformatics/btp616.
85. Petersen TN, Brunak S, von Heijne G, Nielsen H. 2011. SignalP 4.0: discriminating signal peptides from transmembrane regions. Nat Methods 8:785–786. https://doi.org/10.1038/nmeth.1701.
86. Krogh A, Larsson B, von Heijne G, Sonnhammer EL. 2001. Predicting transmembrane protein topology with a hidden Markov model: application to complete genomes. J Mol Biol 305:567–580. https://doi.org/10.1006/jmbi.2000.4315.
87. Priebe S, Kreisel C, Horn F, Guthke R, Linde J. 2015. FungiFun2: a comprehensive online resource for systematic analysis of gene lists from fungal species. Bioinformatics 31:445–446. https://doi.org/10.1093/bioinformatics/btu627.
88. Levasseur A, Drula E, Lombard V, Coutinho PM, Henrissat B. 2013. Expansion of the enzymatic repertoire of the CAZy database to integrate auxiliary redox enzymes. Biotechnol Biofuels 6:41. https://doi.org/10.1186/1754-6834-6-41.
89. Lombard V, Golaconda Ramulu H, Drula E, Coutinho PM, Henrissat B. 2014. The carbohydrate-active enzymes database (CAZy) in 2013. Nucleic Acids Res 42:D490–D495. https://doi.org/10.1093/nar/gkt1178.

ISME

www.nature.com/ismecomms

COMMENT OPEN

Check for updates

RNA-editing in Basidiomycota, revisited

Byoungnam Min[1,2], Baojun Wu[3,4], Jill Gaskell[5], Jiwei Zhang[6], Christina Toapanta[7], Steven Ahrendt[1], Robert A. Blanchette[7], Emma Master[8], Daniel Cullen[5], David S. Hibbett[3]✉ and Igor V. Grigoriev[1,2]✉

ISME Communications; https://doi.org/10.1038/s43705-021-00037-9

In fungi, adenosine-to-inosine (A-to-I) RNA-editing was shown to occur during sexual development and fruiting body formation in filamentous ascomycetes *Fusarium graminearum*, *F. verticillioides*, *Neurospora crassa*, *Sordaria macrospora*, and *Pyronema confluens* (Pezizomycotina) [1, 2], but absent during meiosis in the fission yeast *Schizosaccharomyces pombe* (Taphrinomycotina) [2]. In Basidiomycota, the first RNA-editing report was from *Ganoderma lucidum*, a mushroom-forming species of Polyporales, also during fruiting body formation [3]. Afterwards, Wu et al. reported RNA-editing events in vegetative mycelia of five other species of Polyporales [4, 5]. It was noted that the editing patterns of both *G. lucidum* and the five Polyporales fungi were not only different from the typical A-to-I editing but also showed that transitions (A- > G, G- > A, C- > U, U- > C) were preferred over transversions, leading mainly to synonymous changes in contrast to missense changes found in filamentous ascomycetes [3–5].

Wu et al. predicted RNA-editing sites by aligning transcriptomic reads to the reference genome assembly. However, that approach assumes that the reference assembly is complete, which is rarely the case. The majority of available fungal genome assemblies contain gaps and errors. Even in haploid genomes, multiple nearly-identical DNA regions, for example, transposons or tandem or segmental duplications, can be erroneously collapsed into single fragments, or misassembled. Therefore, RNA reads mapped to such collapsed regions would correspond to distinct genomic regions with 100% coverage and identity and thus would not represent transcripts of the same genes. To avoid this issue, gDNA reads can be aligned and analyzed simultaneously with RNA reads. When a potential RNA-editing site has the same single nucleotide variants as in the gDNA reads alignment, the site should be excluded from candidate RNA-editing sites.

We used this approach to reassess RNA-editing previously reported by Wu et al. for five species of Polyporales [4, 5]. When we compared the polymorphisms derived from the alignment of gDNA reads with those derived from RNA reads, a substantial fraction of these RNA and DNA polymorphisms did match in both the positions and nucleotide substitution types (Fig. 1). From the previously reported 184–1761 RNA-editing sites predicted based on the transcriptome-only analysis [4, 5], 148–1690 (60.68–98.31%) showed matching RNA and DNA polymorphisms and were removed (Table 1). For *Antrodia sinuosa*, DNA and RNA were extracted from different strains [4], which explains more remaining sites (568–923) than in the other four species (8–71).

Some of these remaining candidate sites did not show the single-nucleotide variations when the later version of HISAT alignment was used with intron length restriction (2000 bp). That is because the reads having supported the variations were decoupled and mapped to different regions or were not mapped due to the intron length limitation. In addition, when we searched reads pooled rather than aligned reads, we observed distinct groups of gDNA reads matching the polymorphic RNA reads with 100% identify of the entire length and thus corresponding to different parts of the genome (Table 1). After this multi-step filtering, all but four sites across four species were eliminated. The RNA polymorphism in the remaining four sites can be explained by the differences in isolates used for genome sequencing and for the transcriptomics studies by Wu et al. [4, 5] (Table 2). These polymorphisms were not confirmed in RNA reads used for genome annotation and obtained from the same isolates as DNA. Thus, there is no evidence of RNA editing during the vegetative growth in these five species of Polyporales.

We performed further analyses on how assembly methods can affect detecting RNA/DNA polymorphisms. We reassembled the *Daedalea quercina* genome that previously had been assembled by AllPathsLG [6]. The new assembly was built by SPAdes and resulted in more scaffolds (606 vs. 357), fewer contigs (924 vs. 1025), and slightly smaller assembly size (31.40 vs. 32.74 Mbp). We identified 37 (aspen), 47 (pine), and 45 (spruce) RNA polymorphism sites in the original assembly that correspond to pairs of separate regions in the new assembly, thus eliminating both DNA and RNA polymorphism at those sites. Nevertheless, the new assembly introduced 605 (aspen),

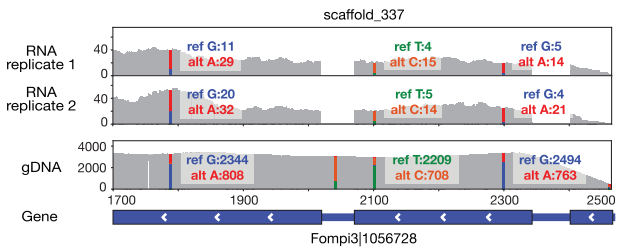

Fig. 1 Previously reported putative RNA-editing sites that show the identical type of polymorphism in the gDNA reads alignment. The RNA samples were extracted from *Fomitopsis pinicola* grown in spruce for ten days.

[1]US Department of Energy Joint Genome Institute, Lawrence Berkeley National Laboratory, Berkeley, CA, USA. [2]Department of Plant and Microbial Biology, University of California, Berkeley, CA, USA. [3]Biology Department, Clark University, Worcester, MA, USA. [4]Statistics and Bioinformatics Group, School of Fundamental Sciences, Massey University, Palmerston North, New Zealand. [5]USDA Forest Products Laboratory, Madison, WI, USA. [6]Department of Bioproducts and Biosystems Engineering, University of Minnesota, St. Paul, MN, USA. [7]Department of Plant Pathology, University of Minnesota, St. Paul, MN, USA. [8]Department of Chemical Engineering and Applied Chemistry, University of Toronto, Toronto, ON, Canada. ✉email: DHibbett@clarku.edu; ivgrigoriev@lbl.gov

Received: 25 May 2021 Revised: 8 July 2021 Accepted: 29 July 2021
Published online: 01 December 2021

Table 1. Previously reported RNA-editing in the five Polyporales fungi.

Species	Sample[a]	Previously reported RNA editing sites	Matching variants in gDNA read alignments[b]	Absent in the new RNA BAMs[c]	Matching variant in gDNA reads[d]	Different RNA and DNA sources
Daedalea quercina L-15889	Aspen-5D	435	421	13	0	1
	Pine-5D	355	347	8	0	0
	Spruce-5D	365	356	8	0	1
Fomitopsis pinicola FP-58527 SS1	Aspen-5D	1568	1510	45	13	0
	Pine-5D	1761	1690	53	18	0
	Pine-10D	753	716	27	9	1
	Pine-30D	1067	1022	34	11	0
	Spruce-5D	1288	1244	32	12	0
	Spruce-10D	901	863	33	5	0
	Spruce-30D	1098	1051	38	9	0
Laetiporus sulphureus 93-53	Aspen-5D	1328	1297	26	5	0
	Pine-5D	1339	1314	21	4	0
	Spruce-5D	1304	1282	19	3	0
Wolfiporia cocos MD-104 SS10	Aspen-5D	184	148	35	0	1
	Pine-5D	212	173	38	1	0
	Spruce-5D	195	153	42	0	0
Antrodia sinuosa[e]	Aspen-5D	1141	698	139	-	304
	Pine-5D	1504	923	229	-	352
	Spruce-5D	936	568	110	-	258

[a]Sample nucleic acids were derived from woody substrates after 5, 10 or 30 days incubation [4, 5].
[b]The number of removed sites where gDNA read alignments show the same single-nucleotide variation.
[c]The number of sites absent in the alignments performed with the latest version of HISAT (v0.1.4-beta used for previous study and v2.1.0 used for this study).
[d]The number of removed sites where polymorphic RNA reads match DNA reads despite lack of alignments into the positions.
[e]Genomic DNA was extracted from LB1 strain while RNA was from LD5-1 strain.

Table 2. Genome and transcriptome data used in this study.

Species	Genome assembly	Genomic reads	Transcriptomes
Antrodia sinuosa[a]	mycocosm.jgi.doe.gov/Antsi1	SRP025451	SRP145284–145291
Fomitopsis pinicola FP-58527 SS1	mycocosm.jgi.doe.gov/Fompi3	SRP004032	SRP140951–140968
Daedalea quercina L-15889	mycocosm.jgi.doe.gov/Daequ1	SRP024551	SRP145276–145283
Laetiporus sulphureus 93-53	mycocosm.jgi.doe.gov/Laesu1	SRP025501	SRP164792–164802
Wolfiporia cocos MD-104 SS10	mycocosm.jgi.doe.gov/Wolco1	SRP002992	SRP145298–145306
Coprinopsis cinerea AmutBmut pab1-1	mycocosm.jgi.doe.gov/Copci_AmutBmut1	SRP053467	SRP179762

[a]Genomic DNA was extracted from LB1 strain while RNA was from LD5-1 strain.

694 (pine), and 704 (spruce) new single nucleotide variants of RNA not found in the old assembly. Thus, the assemblers produce different misassemblies and can potentially suggest new false RNA polymorphisms.

Since the RNA of all five Polyporales species was extracted from mycelium, we extended our analysis to the homokaryon of *Coprinopsis cinerea* (Agaricomycetes, Agaricales) for which transcriptomic data were collected across several developmental stages as reported previously [7]. The samples included vegetative mycelium, secondary hyphal knot, stage 1 primordium, stage 2 primordium, young fruiting body (cap, lamellae, and stipe), and fruiting body (cap + lamellae and stipe). We used both genomic DNA and RNA reads to filter out the false RNA-editing sites derived from potential genome mis-assemblies. As a result, we obtained only two to six RNA variant sites after filtering which can be explained by DNA and RNA extracted from different isolates sequenced in independent studies [7, 8]. Thus, we found no evidence for RNA-editing events in *C. cinerea* during sexual development.

Similar transitions-over-transversions nucleotide patterns of RNA-editing were reported in *Ganoderma lucidum* [3]. The report suggested 8906 RNA-editing sites in *G. lucidum* using analysis of both gDNA and RNA reads, with 94 sites verified with Sanger sequencing [3]. While the reference genome was built by the one of two mating strains (monokaryon), the fruiting-body from which gDNA and RNA were extracted was formed by a dikaryon where two mating strains exist. *G. lucidum* is a heterokaryotic species, making the analysis more challenging because of the ploidy combined with segmental duplications. In order to confirm RNA editing in this species, two haplotypes need to be separated and analyzed independently with proper DNA and RNA reads mapped to each of them to identify haplotype-specific polymorphisms indicating possible mis-assemblies that need to be filtered out in analysis of RNA polymorphisms. This may be quite challenging, but the editing pattern reported in *G. lucidum* was similar to those we corrected in the haploid genomes of Polyporales in that transitions dominate transversions leading to mostly synonymous amino acid changes.

To conclude, we revisited the previously reported RNA-editing in five basidiomycetes, and extended analysis to one more species with transcriptionally profiled developmental stages. The previously reported sites of RNA-editing were artifacts caused by genome misassemblies or variations in the genomes of different isolates from which DNA and RNA were extracted. Furthermore, we suggest reevaluating the RNA-editing in the dikaryotic *G. lucidum* by separate analysis of its two haplotypes. We were also unable to detect RNA-editing patterns in any transcript profiles during development of *C. cinerea*, including sexual development. In short, after reevaluation of available genomes and transcriptomes we did not find evidence of RNA-editing in Basidiomycota.

METHODS AND MATERIALS

We downloaded genomic and transcriptomic read data used in this study from the NCBI database (Table 2). The genome and transcriptome reads were de-duplicated to remove polymerase chain reaction products using Dedupe in BBTools (https://sourceforge.net/projects/bbmap/). Subsequently, the reads were quality controlled using TrimGalore (https://www.bioinformatics.babraham.ac.uk/projects/trim_galore/) by filtering out the reads with bad base quality (<20) and short length (<40). We aligned filtered genomic and transcriptome reads against the corresponding genome assemblies using Bowtie v2.3.5.1 (http://bowtie-bio.sourceforge.net) and HISAT v2.1.0 (http://www.ccb.jhu.edu/software/hisat/), respectively. The candidate RNA-editing sites were detected using JACUSA v1.3.0 [9] (call-2 --filter-flags 1024 --min-mapq1 0 --min-mapq2 0 --pileup-filter S). The variants supported with <20 total mapped reads, <5 or <10% of variant reads, and any sites with matching gDNA variants (>5% variants of mapped reads) were ignored. We used SPAdes v3.13.0 (http://cab.spbu.ru/software/spades) (--careful --cov-cutoff auto) to reassemble *D. quercina* genomic reads. The original and newly assembled genomes were aligned using NUCmer 4.0.0beta2 (http://mummer.sourceforge.net) to find corresponding sites. The RNA reads from the same isolates that DNA reads were generated were downloaded from MycoCosm (https://mycocosm.jgi.doe.gov/) [10].

REFERENCES

1. Liu H, Wang Q, He Y, Chen L, Hao C, Jiang C, et al. Genome-wide A-to-I RNA editing in fungi independent of ADAR enzymes. Genome Res. 2016;26:499–509.
2. Teichert I, Dahlmann TA, Kück U, Nowrousian M. RNA editing during sexual development occurs in distantly related filamentous ascomycetes. Genome Biol Evol. 2017;9:855–68.
3. Zhu Y, Luo H, Zhang X, Song J, Sun C, Ji A, et al. Abundant and selective RNA-editing events in the medicinal mushroom Ganoderma lucidum. Genetics. 2014;196:1047–57.
4. Wu B, Gaskell J, Zhang J, Toapanta C, Ahrendt S, Grigoriev IV, et al. Evolution of substrate-specific gene expression and RNA editing in brown rot wood-decaying fungi. ISME J. 2019;13:1391–403.
5. Wu B, Gaskell J, Held BW, Toapanta C, Vuong T, Ahrendt S, et al. Substrate-specific differential gene expression and rna editing in the brown rot fungus Fomitopsis pinicola. Appl Environ Microbiol. 2018;84.e00991–18.
6. Nagy LG, Riley R, Tritt A, Adam C, Daum C, Floudas D, et al. Comparative genomics of early-diverging mushroom-forming fungi provides insights into the origins of lignocellulose decay capabilities. Mol Biol Evol. 2016;33:959–70.
7. Krizsán K, Almási É, Merényi Z, Sahu N, Virágh M, Kószó T, et al. Transcriptomic atlas of mushroom development reveals conserved genes behind complex multicellularity in fungi. Proc Natl Acad Sci U S A. 2019;116:7409–18.
8. Muraguchi H, Umezawa K, Niikura M, Yoshida M, Kozaki T, Ishii K, et al. Strand-specific RNA-Seq analyses of fruiting body development in Coprinopsis cinerea. PLoS One. 2015;10:e0141586.
9. Piechotta M, Wyler E, Ohler U, Landthaler M, Dieterich C. JACUSA: site-specific identification of RNA editing events from replicate sequencing data. BMC Bioinformatics. 2017;18:7.
10. Grigoriev IV, Nikitin R, Haridas S, Kuo A, Ohm R, Otillar R, et al. MycoCosm portal: gearing up for 1000 fungal genomes. Nucleic Acids Res. 2014;42:D699–704.

ACKNOWLEDGEMENTS

This work was supported by National Science Foundation awards IOS-1456777 (to DSH), IOS-1456548 (to RAB), IOS-1456958 (to IVG), and DEB-1457721 (to DC). The work conducted by the U.S. Department of Energy Joint Genome Institute, a DOE Office of Science User Facility, is supported by the Office of Science of the U.S. Department of Energy under Contract No. DE-AC02-05CH11231.

AUTHOR CONTRIBUTIONS

BM, BW, DSH and IVG conceptualized the study. BM and BW conducted analyses. BM, DSH, and IVG wrote the paper with input from JG, JZ, CT, SA, RAB, EM, and DC.

COMPETING INTERESTS

The authors declare no competing interests.

ADDITIONAL INFORMATION

Correspondence and requests for materials should be addressed to David S. Hibbett or Igor V. Grigoriev.

AMERICAN SOCIETY FOR MICROBIOLOGY | Microbiology Resource Announcements

OMICS DATA SETS

Proteome of the Wood Decay Fungus *Fomitopsis pinicola* Is Altered by Substrate

Grzegorz Sabat,[a] Steven Ahrendt,[b,c] Baojun Wu,[d] Jill Gaskell,[e] Benjamin W. Held,[f] Cristina Toapanta,[f] Thu V. Vuong,[g] Anna Lipzen,[b] Jiwei Zhang,[h] Jonathan S. Schilling,[h,i] Emma Master,[g] Igor V. Grigoriev,[b,c] Robert A. Blanchette,[f] David S. Hibbett,[d] Jennifer Bhatnagar,[j] Daniel Cullen[e]

[a]University of Wisconsin-Madison Biotechnology Center, Madison, Wisconsin, USA
[b]Department of Energy Joint Genome Institute, Berkeley, California, USA
[c]Department of Plant and Microbial Biology, University of California, Berkeley, Berkeley, California, USA
[d]Biology Department, Clark University, Worcester, Massachusetts, USA
[e]USDA Forest Products Laboratory, Madison, Wisconsin, USA
[f]Department of Plant Pathology, University of Minnesota, St. Paul, Minnesota, USA
[g]Department of Chemical Engineering and Applied Chemistry, University of Toronto, Toronto, Ontario, Canada
[h]Department of Bioproducts and Biosystems Engineering, University of Minnesota, St. Paul, Minnesota, USA
[i]Plant and Microbial Biology, University of Minnesota, St. Paul, Minnesota, USA
[j]Department of Biology, Boston University, Boston, Massachusetts, USA

ABSTRACT The brown rot fungus *Fomitopsis pinicola* efficiently depolymerizes wood cellulose via the combined activities of oxidative and hydrolytic enzymes. Mass spectrometric analyses of culture filtrates identified specific proteins, many of which were differentially regulated in response to substrate composition.

Two-liter flasks containing 250 mL of basal salt medium were supplemented with 1.25 g of ground and sieved (number 10 screen) quaking aspen (*Populus tremuloides*), loblolly pine (*Pinus taeda*), or white spruce (*Picea glauca*) wood as the sole carbon source, as described (1, 2). The medium was inoculated with *Fomitopsis pinicola* strain FP-58527 (= *Fomitopsis schrenkii* [3]) and placed on a rotary shaker (150 rpm). After 5 days of incubation at 22°C to 24°C, cultures were filtered through Whatman GF/C filters followed by Corning 0.22-μm polystyrene filters (catalog number 430531). Filtrate proteins were precipitated with 10% (wt/vol) trichloroacetic acid and purified (4). Three replicated cultures were harvested for each wood species.

Nano-liquid chromatography-tandem mass spectrometry (nano-LC-MS/MS) was used to identify proteins (5–7). Equal amounts of total protein per sample were digested with trypsin/LysC and purified with OMIX C_{18} SPE cartridges (Agilent Technologies), and 2 μg was loaded for nano-LC-MS/MS analysis, using an Agilent 1100 nanoflow system (Agilent Technologies) connected to a hybrid linear ion trap-Orbitrap mass spectrometer (LTQ-Orbitrap Elite; Thermo Fisher Scientific) equipped with an EASY-Spray electrospray source. Chromatography of peptides prior to MS analysis was accomplished using a capillary emitter column (PepMap C_{18} column, 3 μm, 100 Å, 150 by 0.075 mm; Thermo Fisher Scientific), onto which 2 μl of purified peptides was automatically loaded. The nano-LC system delivered solvents as described (4), and survey MS scans were acquired in the Orbitrap mass spectrometer with a resolution of 120,000, followed by MS2 fragmentation of the 20 most intense peptides detected in the MS1 scan from *m/z* 380 to 1800, with redundancy limited by dynamic exclusion. Raw MS/MS data were converted to the mgf file format using MSConvert (ProteoWizard) for downstream analysis. Resulting mgf files were used to search against forward and decoyed-reversed *F. pinicola* protein databases via the Joint Genome Institute (JGI) portal (https://mycocosm.jgi.doe.gov/Fompi3/Fompi3.info.html),

Editor Antonis Rokas, Vanderbilt University

Address correspondence to Daniel Cullen, dcullen@wisc.edu.
The authors declare no conflict of interest.

Received 10 June 2022
Accepted 27 July 2022
Published 15 August 2022

with a list of common laboratory contaminants (available at https://reprint-apms.org/?q=chooseworkflow) to establish the false discovery rate (FDR) (37,222 total entries) using an in-house Mascot search engine v2.2.07 (Matrix Science) with variable methionine oxidation and asparagine and glutamine deamidation and fixed cysteine carbamidomethylation. Scaffold v4.7.5 (Proteome Software Inc., Portland, OR) was used for spectrum-based quantification. Peptide identifications were accepted if they could be established at >80.0% probability to achieve an FDR of <1.0% by the Scaffold local FDR algorithm. Protein identifications were accepted if they could be established at >99.0% probability to achieve an FDR of <1.0% and contained at least 2 identified peptides. Protein probabilities were assigned by the Protein Prophet algorithm (8). Proteins that contained similar peptides and could not be differentiated based on MS/MS analysis alone were grouped to satisfy the principles of parsimony.

A total of 200 proteins were confidently identified, of which 56 were carbohydrate-active enzymes (CAZymes) (9). Analysis of variance (ANOVA) revealed ≥2-fold accumulation of 38 proteins; of those, 30 were more abundant in aspen than in pine. These data will serve as a useful resource for studying the influence of substrate composition on protein secretion by *F. pinicola*.

Data availability. The MS proteomic data and supplemental ANOVA results have been deposited in the ProteomeXchange through PRIDE with the identifier PXD033887 (http://www.ebi.ac.uk/pride/archive/projects/PXD033887).

ACKNOWLEDGMENTS

Research was supported by NSF Division of Environmental Biology grants 1457695 and 1457721 to J.B. and D.C., respectively.

REFERENCES

1. Wu B, Gaskell J, Held BW, Toapanta C, Vuong TV, Ahrendt S, Lipzen A, Zhang J, Schilling JS, Master E, Grigoriev IV, Blanchette RA, Cullen D, Hibbett DS. 2021. Retracted and republished from: "Substrate-specific differential gene expression and RNA editing in the brown rot fungus *Fomitopsis pinicola*." Appl Environ Microbiol 87:e00329-21. https://doi.org/10.1128/AEM.00329-21.
2. Gaskell J, Blanchette RA, Stewart PE, BonDurant SS, Adams M, Sabat G, Kersten P, Cullen D. 2016. Transcriptome and secretome analyses of the wood decay fungus *Wolfiporia cocos* support alternative mechanisms of lignocellulose conversion. Appl Environ Microbiol 82:3979–3987. https://doi.org/10.1128/AEM.00639-16.
3. Haight JE, Nakasone KK, Laursen GA, Redhead SA, Taylor DL, Glaeser JA. 2019. *Fomitopsis mounceae* and *F. schrenkii*: two new species from North America in the *F. pinicola* complex. Mycologia 111:339–357. https://doi.org/10.1080/00275514.2018.1564449.
4. Bhatnagar JM, Sabat G, Cullen D. 2019. The foliar endophyte *Phialocephala scopiformis* DAOMC 229536 proteome when grown on wood used as the sole carbon source. Microbiol Resour Announc 8:e01280-18. https://doi.org/10.1128/MRA.01280-18.
5. Hori C, Ishida T, Igarashi K, Samejima M, Suzuki H, Master E, Ferreira P, Ruiz-Duenas FJ, Held B, Canessa P, Larrondo LF, Schmoll M, Druzhinina IS, Kubicek CP, Gaskell JA, Kersten P, St John F, Glasner J, Sabat G, Splinter BonDurant S, Syed K, Yadav J, Mgbeahuruike AC, Kovalchuk A, Asiegbu FO, Lackner G, Hoffmeister D, Rencoret J, Gutierrez A, Sun H, Lindquist E, Barry K, Riley R, Grigoriev IV, Henrissat B, Kues U, Berka RM, Martinez AT, Covert SF, Blanchette RA, Cullen D. 2014. Analysis of the *Phlebiopsis gigantea* genome, transcriptome and secretome provides insight into its pioneer colonization strategies of wood. PLoS Genet 10:e1004759. https://doi.org/10.1371/journal.pgen.1004759.
6. Fernandez-Fueyo E, Ruiz-Duenas FJ, Ferreira P, Floudas D, Hibbett DS, Canessa P, Larrondo LF, James TY, Seelenfreund D, Lobos S, Polanco R, Tello M, Honda Y, Watanabe T, Ryu JS, Kubicek CP, Schmoll M, Gaskell J, Hammel KE, St John FJ, Vanden Wymelenberg A, Sabat G, Splinter BonDurant S, Syed K, Yadav JS, Doddapaneni H, Subramanian V, Lavin JL, Oguiza JA, Perez G, Pisabarro AG, Ramirez L, Santoyo F, Master E, Coutinho PM, Henrissat B, Lombard V, Magnuson JK, Kues U, Hori C, Igarashi K, Samejima M, Held BW, Barry KW, LaButti KM, Lapidus A, Lindquist EA, Lucas SM, Riley R, Salamov AA, et al. 2012. Comparative genomics of *Ceriporiopsis subvermispora* and *Phanerochaete chrysosporium* provide insight into selective ligninolysis. Proc Natl Acad Sci U S A 109:5458–5463. https://doi.org/10.1073/pnas.1119912109.
7. Hori C, Gaskell J, Cullen D, Sabat G, Stewart PE, Lail K, Peng Y, Barry K, Grigoriev IV, Kohler A, Fauchery L, Martin F, Zeiner CA, Bhatnagar JM. 2018. Multi-omic analyses of extensively decayed *Pinus contorta* reveal expression of a diverse array of lignocellulose-degrading enzymes. Appl Environ Microbiol 84:e01133-18. https://doi.org/10.1128/AEM.01133-18.
8. Nesvizhskii AI, Keller A, Kolker E, Aebersold R. 2003. A statistical model for identifying proteins by tandem mass spectrometry. Anal Chem 75:4646–4658. https://doi.org/10.1021/ac0341261.
9. Lombard V, Golaconda Ramulu H, Drula E, Coutinho PM, Henrissat B. 2014. The Carbohydrate-Active Enzymes database (CAZy) in 2013. Nucleic Acids Res 42:D490–D495. https://doi.org/10.1093/nar/gkt1178.